Minireview

Modeling the lung: Design and development of tissue engineered macro- and micro-physiologic lung models for research use

Joan E Nichols[1,2,3], Jean A Niles[1], Stephanie P Vega[1,2], Lissenya B Argueta[1,2], Adriene Eastaway[1,3] and Joaquin Cortiella[4]

[1]University of Texas Medical Branch, Department of Internal Medicine, Division of Infectious Diseases, Galveston, TX 77555-0435, USA; [2]University of Texas Medical Branch, Department of Microbiology and Immunology, Galveston, TX 77555-0435, USA; [3]University of Texas Medical Branch, School of Medicine, Galveston, TX 77555-0435, USA; [4]University of Texas Medical Branch, Department of Anesthesiology, Galveston, TX 77555-0435, USA

Corresponding author: Joan E Nichols. Email: jnichols@utmb.edu

Abstract

Respiratory tract specific cell populations, or tissue engineered *in vitro* grown human lung, have the potential to be used as research tools to mimic physiology, toxicology, pathology, as well as infectious diseases responses of cells or tissues. Studies related to respiratory tract pathogenesis or drug toxicity testing in the past made use of basic systems where single cell populations were exposed to test agents followed by evaluations of simple cellular responses. Although these simple single-cell-type systems provided good basic information related to cellular responses, much more can be learned from cells grown in fabricated microenvironments which mimic *in vivo* conditions in specialized microfabricated chambers or by human tissue engineered three-dimensional (3D) models which allow for more natural interactions between cells. Recent advances in microengineering technology, microfluidics, and tissue engineering have provided a new approach to the development of 2D and 3D cell culture models which enable production of more robust human *in vitro* respiratory tract models. Complex models containing multiple cell phenotypes also provide a more reasonable approximation of what occurs *in vivo* without the confounding elements in the dynamic *in vivo* environment. The goal of engineering good 3D human models is the formation of physiologically functional respiratory tissue surrogates which can be used as pathogenesis models or in the case of 2D screening systems for drug therapy evaluation as well as human toxicity testing. We hope that this manuscript will serve as a guide for development of future respiratory tract model systems as well as a review of conventional models.

Keywords: Engineered lung models, engineered organ models, 3D lung models, physiologic lung as a model, upper respiratory tract models, micro-physiologic lung

***Experimental Biology and Medicine* 2014; 239: 1135–1169. DOI: 10.1177/1535370214536679**

Introduction

In the past the most widely used experimental models for physiologic and pathologic studies of the lungs included static two-dimensional (2D) cell culture systems. Lung models represented by tissue culture plate grown cell cultures do not always accurately reflect the interactions between cells or within tissue interfaces in the macro-environment of the lung.[1,2] Although simple single-cell-type systems provide good basic information related to cellular responses much more can be learned from human models which allow for more natural interactions between cells or tissues. This is especially important for the design of studies related to human disease or pathogenesis of respiratory pathogens. Using techniques for the development of specialized 2D chambers which mimic tissue microenvironments or 3D tissue engineered human lung constructs allows for the generation of models in which cell types may be selectively added to create complex systems which mimic very specific physiological interactions within the lung. These types of model systems, unlike *in vivo* animal models, also allow us to deconstruct complex mechanisms of pathogenesis in order to simplify the study of individual cellular components, immune factors, or effector molecules involved in lung disease. Throughout the years, various models have been developed to study physiological responses of the lungs and pathological changes in lung disease. The differences between models depend upon what region of the lungs the engineered system is attempting to mimic and the pathological

condition being studied. Models have already been created which allowed us to examine cellular mechanisms of lung progenitor cell responses, critical cues in lung development or responses of respiratory tissues to extracellular matrix (ECM) and mechanical stimuli. Development of better models in the future will revolutionize the way we study human biology, physiology, and disease development.

Construction of human trachea, trachea–lung, or distal lung models for research use

Production of tissue models that will be used to mimic tissue or organ systems physiology or responses requires the selection of an appropriate (1) scale for the model, (2) cell source, (3) support scaffold, (4) culture support system, and (5) method for validation and assessment. Before a respiratory tract model can be constructed, for example, the region of the system to be modeled must be carefully considered. Respiratory tract models need to accurately reflect morphological structures, functional features, and cell phenotypes found in human trachea, bronchi, bronchioles, or distal lungs. When designing any human tissue model, it is important to determine what parameters must be reconstituted in order to create a model that will be used to study physiology, toxicology, pathology, or infectious diseases. For the development of respiratory tract models which include both trachea (upper respiratory tract) and lung models (lower respiratory tract) consideration of the above parameters is extremely important. Examination of the influence of ECM of the entire respiratory tract on embryonic stem cell (ESC) differentiation necessitated the use of a whole trachea–lung.[3] Other models may focus on specific regions of the upper or lower respiratory tract alone. It is important to consider the unique anatomy and physiology of the human respiratory tract when creating human tissue mimics so that we create models which increase our understanding of how diseases affect the lungs or help us to identify new targets for drug development to aid in treating lung diseases in the future.

Size matters

When designing a tissue model, the size of the system matters a great deal. To replicate human physiology and drug responses it is critical that each type of tissue system has the correct relative size to model desired responses.[4] Estimating the number of cells necessary for creation of a model is a difficult task. Estimates based on allometric scaling for the distal lung or alveolar regions suggest that a μlung (alveolus) would contain approximately 184,000 cells.[4] Microphysiologic systems such as organ-on-a chip models of the alveolar region of the lung based on allometric scaling require few cells (less than a million) and can be maintained in chambers supported by microfluidic systems which provide fresh media and growth factors into a cell chamber and remove waste products from the system. These μlung systems can be used to evaluate basic changes in cell viability, apoptosis induction, or may even be used to design simple pathological models.[5] Examination of cell products may be limited in these μlung models due to the small chamber size and microfluidic perfusion rates.

Modeling of complex human disease pathologies on a larger scale may require larger numbers of cells or combinations of integrated tissues in order to support development of a specific physiologic or pathologic response in the model. Larger culture systems referred to as human organ construct (HoC)[4] models would require use of heterogeneous mixtures of numerous cell phenotypes, the number of which depends on the human disease one is attempting to model. Engineering of 3D tissue models starts with generating healthy physiologically functioning tissue and requires a holistic and robust understanding of cellular and tissue responses. The size of a model may be limited by diffusion capacity because of a lack of vascularization or transport systems necessary for supporting the natural metabolic processes of cells and tissues. Microfluidic support systems can be used to manage μlung cultures but larger HoC may require design and production of specialized fluidic systems or development of vascularized tissue that can be interfaced with fluidic support.

The critical cell types required to facilitate development of specific responses or pathologies must also be taken into consideration and, for the lung, often requires inclusion of more than alveolar epithelial (AEC) type I and II cells. Generation of milli-human distal lung models to examine complex components of influenza A pathogenesis requires the inclusion of approximately 1–2 million of type I and II AEC, fibroblasts, 1 million endothelial cells, 0.5–1 million smooth muscle cells, and 0.5–1 million leukocytes (unpublished data from the authors). HOC systems often contain 6–10 million cells (unpublished data from the authors). Biofabrication of macro-physiologic model systems to study diseases such as diffuse alveolar damage (DAD) would require at the minimum the presence of type I and II AEC, macrophages, neutrophils, and endothelial cells. The number of cells of each type which will be required to induce DAD is difficult to estimate and often estimations of required cell numbers cannot be determined until after generation of physiologic lung tissue and examination of the responses of the tissue in an integrated metabolic HoC system.

What cell types can be used in modeling the respiratory tract

Selection of an appropriate cell source is one of the greatest hurdles in developing engineered lung models. Primary human tracheal–bronchial cells and lung primary AECs generally function as the ''gold standard'' to which all other cell types are compared. Table 1 lists some of the main cell types that have been used to engineer either trachea–bronchi or distal lung models as well as some of the advantages/disadvantages of each cell type. Problems related to use of primary cells include the difficulty in obtaining human tissue as well as isolation of cells with low viability due to transport problems or delays in acquisition of viable human tissues and in the isolation of cells. One way to improve viability of lung tissue is to maintain procured lungs on a Harvard apparatus system until cells

Table 1 Common cell types used in the generation of lung tissue models

Cell Type	(+) Advantages	(−) Disadvantages
Primary NHBE Normal human bronchial/ tracheal epithelial cells[6–8]	– Can manipulate growth and differentiation through use of epinephrine and TGF-β. – Can be immortalized through expression of hTERT and Cdk4 to serve as a model to study molecular pathogenesis of lung cancer.	– Must be obtained within 12 h postmortem though it becomes progressively more difficult to establish a culture should the postmortem interval exceed 6 h. – Alternative method to obtain cells is via bronchoscopy though it offers a much lower yield. – Potential for microbial contamination.
HBSM(C)/HASM Human bronchial/airway smooth muscle cells[9–12]	– Used in 3D models to study asthma on cross-sectioned airway segments. – Presence of C3a and C5a receptors makes these cells useful in modeling sepsis as well as asthma. – Express transcripts for IL-4 α, IL-13 R α I, and IL-13 R α II and high affinity for IgE. – Capable of influencing airway inflammation and growth factors via the production of prostanoids and chemokines (IL-11, IL-6, IL-8, RANTES, eotaxin). – Ability to modify airway modeling by the production of matrix-degrading enzymes (metalloproteinases). – Synthesize VEGF protein.	– Underlying factor(s) of hyperplasia/hypertrophy of these cells remain unidentified. – Inevitable phenotypic modulations occur in culture. – Contaminating epithelial cells; difficulty in obtaining a pure population.
16HBE14o- Human bronchial epithelial cell line[13–16]	– Forms polarized cell layers *in vitro*. – Provide a discriminatory barrier to solute transport (suitable barrier properties by day 6 in culture). – Grown on monofibrillar collagen because of ease of application, reproducibility, and uniformity of layers. – Express drug transport systems that are also present in the human bronchus *in vivo* (P-gp, LRP, and Cav-1). – Retains many features of differentiated bronchial epithelial cells. – Form tight junctions (ZO-1 and occludin positive stains).	– How culture conditions affect expression of airway-specific transport mechanisms is not fully understood.
Calu-3 Human submucosal adenocarcinoma cell line[17–21]	– Readily available cell line. – Well-characterized cell line. – Differentiates into monolayers of polarized cells of varying phenotypes in 3D. – Their morphological features, presence of transport systems, efflux pumps, and metabolic pathways allows for qualitative prediction of the fate of drugs exposed to the lung. – Impact airway surface liquid, mucins, etc – Can be grown at air–liquid interface. – Functional intracellular tight junctions mediate monolayer restrictiveness (observed by staining of the ZO-1 protein), thus high TEER values. – Maximum TEER values were achieved around days 10–14 after monolayers were seeded onto collagen-coated filter membranes. – Exhibit passive diffusion and to a lower degree also low-affinity mediated transport of antibiotics at the apical and basolateral cell membranes.	– Noninducible P450 enzymes. – The transport of Gly-Ser and other peptide substrates as well as insulin requires further investigation before use for pulmonary drug absorption models. – Little is known about how these cells secrete multidrug-resistant proteins (MRPs).
Primary AECs Human alveolar epithelial type I and II mix of primary cells[22–24]	– Used as the gold standard for comparison of other cell types. – Accurately demonstrate *in vivo* behavior. – Controllable cell division. – Used to validate the model. – Capable of TGF-ß1 induced epithelial–mesenchymal transition in culture. – Metabolically active. – Harbor necessary cell surface receptors for signaling.	– Time consuming isolation. – High risk for bacterial or fungal contamination following isolation. – Never 100% pure isolation. – Financial cost for reagents used in isolation (collagenase, dispase, etc.). – Cells cannot be passaged repeatedly. – Cells can be growth dependent and need to be maintained at an adequate seeding density.

(continued)

Table 1 Continued

Cell Type	(+) Advantages	(−) Disadvantages
A549 Human lung adenocarcinoma alveolar basal cell line[25–27]	– Consistent AECII metabolic/transport properties. – They are genetically homogenous. – -Can be grown in large quantities. – They produce confluent monolayers with AECII morphology and lamellar bodies present. – Has inducible P450 enzymes (IA1 and IIB6) consistent with *in vivo* AECIIs.	– Monolayers formed are leaky because they lack tight junctions. – Very low trans-epithelial electrical resistance (TEER) values which make it difficult to measure the transport of low molecular weight molecules. – Cells are genetically and phenotypically homogenous.
HUVEC Human umbilical vein endothelial cells[28–31]	– Constitutively express appropriate cell markers (ICAM-1, PECAM-1, MHC I). – TNFα inducible expression of adhesion molecules (VCAM-1, E-selectin). – All major signaling pathways present/intact. – Proper cytokine responses. – Isolation/culture methods exist. – Form a monolayer of density-inhibited cells with a cobblestone-like morphology when grown on Matrigel diluted 1:3 in serum-free cell culture medium in a 24-well plate. – Appropriate expression of von Willebrand factor (vWF).	– Low yields when isolated. – Possibility of contamination with other cell types at isolation. – Can be difficult to culture. – Can express altered expression of endothelial markers during *in vitro* propagation.
HuLECs/HPMECs Primary human (lung/pulmonary) microvascular endothelial cells[32–34]	– Published isolation methods exist. – Purity can be achieved using a highly specific selective marker, Ulex Europaeus Agglutin-1 (UEA-1). – There is high constitutive production of vWF, PECAM-1/CD31. – Cells express two vascular endothelial growth factor receptors Flt-1 and KDR. – *In vitro* responses to TNFα, LPS, and IL-1β by induction of cell adhesion molecules (ICAM-1/CD54, VCAM-1/CD106, and E-selectin) and secretion of proinflammatory cytokines (IL-6, IL-8, MCP-1, and GM-CSF) via AEC interactions. – Capable of responding to infectious agents via Toll-like receptors expressed on their cell surface.	– Need to prevent overgrowth. – Contaminating fibroblasts, pericytes, smooth muscle cells. – Require considerable cell expansion, manipulation, and *in vitro* culture time.
MRC-5 Human fetal lung fibroblast cell line[35,36]	– Grow as adherent cells in culture. – Exhibit fibroblast morphology. – Well-characterized and well-defined nontumorigenic phenotype. – Widely used human diploid cell line.	Develop into fibroblasts but no other cell types.
W1-38/CCL-75 Human fetal lung fibroblast cell line[37–39]	– Grow as adherent cells in culture. – Can be used to test antivirals. – Well-characterized and well-defined nontumorigenic phenotype. – Widely used human diploid cell line.	Develop into fibroblasts but no other cell types.
hESC – Human embryonic stem cells[40]	– Ability to differentiate into progeny with differentiated phenotypes (pluripotency). – Production of all normal lung cell types. – Cells provide a renewable source for population of models. – Potential for self-renewal and plasticity is excellent.	– Cells can be highly unstable. – In culture cells often form teratomas. – There are indications of genetic instability after prolonged culture time (aneuploidy). – There can be frequent epigenetic errors (SSEA-4/STAT4 expression, TGFβ signaling, telomere length, collagen down-regulation, etc.).
iPS Induced pluripotent stem cells[41–44]	– Circumvents the difficulties faced when generating patient- or disease-specific embryonic stem cells. – Express many undifferentiated embryonic cell-marker genes at equivalent or elevated levels: OCT3/4, SOX2, NANOG, GDF3, FGF4, ESG1, DPPA2, DPPA4, and hTER; thus these cells have	– Cell production using retrovirus transduction to force expression of c-Myc, Klf4, Oct 3/4, and Sox2–can lead to transcription of undesired genes and an increased risk of tumor formation. – Existing alternative methods that do not utilize transgenes often have a low yield.

(continued)

Table 1 Continued

Cell Type	(+) Advantages	(−) Disadvantages
	high flexibility. – High telomerase activity and exponential proliferation for at least 4 months with a doubling time equivalent to human embryonic cells (~46 h). – Ability to form three germ layers *in vitro* observed by embryoid body formation. – Lineage-directed differentiation has been limited and at low efficiency to lung lineages.	– Cell programming is dependent upon the original cell type being transformed. – Cell generation efficiency remains low despite efforts to improve yield.

AEC: alveolar epithelial cell; BAL: bronchiolar alveolar lavage; BMPR2: bone morphogenetic protein receptor-2; ECM: extracellular matrix; HLA: human leukocyte antigen; IFN: interferon; IL: interleukin; IT: intratracheal; IV: intravenous; MIP: macrophage inflammatory protein; NHBE: normal human bronchial epithelium; PAH: pulmonary artery hypertension; PASMC: pulmonary artery smooth muscle cell; PF: pulmonary fibrosis; PMN: polymorphonuclear leukocyte; ROS: reactive oxygen species; 3D: three-dimensional; TNF: tumor necrosis factor; VEGFR: vascular endothelial growth factor receptor.

can be isolated.[46] Disadvantages of using transformed cell lines are related to the loss of normal cell responses due to the fact that these cells were isolated originally from human cancers and therefore exhibit an increased growth rate and are able to divide indefinitely.

Simple physiologic models of the lung have been produced from many of these cell types and provided basic information related to epithelial cell attachment, interactions with scaffold materials, and production of ECM components or protein products. Lung models have been created using mixtures of primary type I and II AECs,[45] transformed cell lines such as A549,[46–53] fetal lung cells (FLCs),[49,54–60] somatic lung progenitor cells (SLPCs), as well as ESCs[3,45,61,62] (Table 1). For generation of human lung models, human microvasculature has been provided by use of human umbilical vein endothelial cells[48,49,63] or primary human pulmonary endothelial cells.[5,47] Selection of the cell type to be used in production of a lung model therefore depends on the type of model being constructed (physiologic, toxological, pathological, or disease). When engineering an infectious disease model, for example, cell selection must consider use of phenotypes of cells that are permissive to a specific viral pathogen and support viral replication. For example in humans, influenza viruses replicate in the ciliated epithelium of conducting airways, which consists of several distinct cell types with different functions found in different regions of the respiratory tract.[64] In order to produce a 3D upper respiratory model to study human influenza A infection, differentiated cultures of human tracheobronchial epithelium (HTBE) should be used. The HTBE should resemble human *in vivo* airway epithelium in that it is pseudostratified and polarized and the model should contain ciliated, secretory, and basal cells, with morphologic, physiologic, and functional similarity to normal human tissues.[64]

Although human embryonic stem cells (hESC)[65] and induced pluripotent stem cells (iPSC)[66] have been used to generate lung epithelial cells neither cell type has been used in the production of lung tissue or to generate physiologic models of the lung. For the generation of standardized lung models, production of lung tissue from cells derived from renewable sources such as hESC or human iPSC is appealing, since it offers the possibility of production of replicate cultures and exposure to toxins or microbial pathogens under standardized conditions. Although models of airway generated from hESC have not been realized, the capacity of murine ESC to generate airway epithelia[61] or lung tissue[3] has been demonstrated. Generation of upper and lower respiratory tract tissues including ciliated epithelial cells, Clara cells, and production of type II AECs expressing surfactant protein-A (SP-A) with production and secretion of surfactant protein-A from murine embryonic stem cell (mESC) was described by Cortiella *et al*.[3] Recent production of type I and II AEC from human iPS cells[67] and derivation of lung progenitors from patient-specific cystic fibrosis iPS cells[68] have been important steps in the production of differentiated lung epithelium for disease modeling with potential use in the design of models for testing of patient-specific therapies for cystic fibrosis or other lung diseases in the future.[69]

Selection of an appropriate scaffold

Selection of an appropriate scaffold to support production of 3D tissue requires the use of materials which meet the specific needs of the model being generated. For development of lung tissue the scaffolding must provide the framework necessary to support cell attachment, cell growth, and tissue formation and in some instances possess the elasticity of normal lung. Use of scaffold materials to engineer lung tissue has been reviewed previously by the authors and will not be discussed at length.[69–71] In brief variable degrees of success have been achieved in the development of both natural and synthetic hydrogels as scaffolds for engineering of lung model systems. A number of hydrogels have been produced which are structurally similar to the ECM of many tissues. Hydrogels can be designed to be environmentally sensitive and react to small changes in light,[50] pH, temperature, or even protein concentration making them good scaffolds to use when producing environmentally responsive models. Both synthetic and natural hydrogels have been used to produce engineered lung models. Hydrogels such as Matrigel,[45,55,57] collagen I[72,73] and Pluronic F-127 (PF-127)[62] as well as hydroxyethyl methacrylate-alginate-gelatin (HAG)[74] have all been used to support development of lung models. Scaffolds that have been used to generate trachea or lung models also include

Engelbreth-Holm-Swarm (EHS) tumor membrane,[54] Gelfoam, Matrigel, collagen I, polyglycolic acid (PGA), PF-127 hydrogel, poly-lactic-*co*-glycolic acid (PLGA),[57] and poly-L-lactic-acid (PLLA)[57] and HAG cryogel scaffold which is a mixture of polysaccharide (alginate) and protein (gelatin). All of these scaffolds have been used with some success to support the generation of lung tissue *in vitro*. Development of physiologic models of the lung has also been accomplished using whole trachea–lung mouse or rat acellular (AC) scaffolds.[3,49,53,60,75] In these studies whole AC trachea–lung scaffolds were reconstituted with mouse[60] or rat FLCs[49,75] or with mESCs.[3] Table 2 lists most of the existing upper and lower respiratory tract models as well as the scaffold material, cell types, and culture support systems used in creation of each model. AC natural scaffolds are composed of the ECM secreted by the resident cells of the tissue or organ from which they are produced. Techniques used for tissue and whole organ decellularization have been reviewed, including descriptions of solvents, detergents, physical agents, and enzymes.[76] The first study of human AC lung to support cell adherence described using strips of AC alveolar matrix seeded with rat type II AECs to examine the influence of ECM on cell attachment and morphology. The AC scaffold described contained collagen I, II, IV, and V as well as laminin and fibronectin.[77] Glycosoaminoglycans were also present as indicated by immunostaining. Rat type II AEC seeded on the human AC lung scaffold took on some of the morphological characteristics of type I AECs. Models to examine remodeling of ECM require scaffolds that are biomodifiable and contain one or more of the normal components of lung ECM such as collagen I.

Design and selection of respiratory model platforms or support systems

Most of the existing engineered trachea or lung models were created as physiological systems without any thought regarding long-term fluidic support of the tissue. Simple platforms utilized to support tissue development include tissue culture plates or 12-, 24-, or 96-well plate systems (Figure 1(a)), and slide chamber systems (Figure 1(c)). Most researchers use these simple culture platforms to develop and maintain respiratory tract epithelial cells or lung equivalents (Table 2). Transwell plates (Corning, Tewksbury, MA) allow for coculture of cells or development of hanging drop suspensions of cells or cell constructs. Slide-based culture chambers are also used but do not allow media exchange or long-term support of developing tissues (Figure 1(b) and (c)). Use of these platforms is limited in that replenishment of media and removal of wastes is not automated and must be monitored and maintained manually. Automation of media transfer and sampling would facilitate the production of large quantities of cells, but would also impact how 2D and 3D cells and tissues are generated, how organs and tissues can be consistently produced and standardized, and how they will be used in drug screening assays in the future.

Perfusion bioreactors have been developed in various configurations and capacities for different biotechnological applications yet their application in lung growth or culturing has been limited. The use of bioreactors (Figure 1(d)) for support of engineered lung tissue offers several potential advantages as compared to static 2D plate or 12-, 24-, or 96-well plate culture. Bioreactors allow (1) uniform and efficient mixing coupled with precise control over material transfer rates; (2) regulation of shear stress within the culture vessel; (3) maintenance of constant pH, gas partial pressures (pO_2, pCO_2), and nutrient levels; and (4) control strategies which can match the changing needs of a growing construct over the entire duration of its cultivation. Bioreactor chambers come in a variety of sizes (from 1 to 500 mL) and have been shown to maintain tissue constructs for 21 days in culture enabling long-term perfusion culture of cells in a 3D environment.[3]

More recent design and execution of microfluidic based platforms for single cell analysis, as reviewed by Lin and Singh, or that allow for examination of small-scale evaluation of cell-to-cell interactions as reviewed by Delamarch *et al.*, provide support for small numbers of cells or small 3D tissue constructs (Figure 1(e)).[78,79] These micro-culture systems have been designed to meet the needs of high throughput preclinical screening of tissue responses to drugs or potentially toxic materials. Production of compartmentalized micro-devices uses techniques such as photolithography,[80–82] microprinting,[80] and replica molding[80,81] to generate the chambers and fluidic channels to support cell attachment and growth (Figure 2). The example shown in Figure 1(e) of this review shows a replica molded multichamber system produced from polydimethylsiloxane (PDMS) which is one of the fundamental materials used in the fabrication of microfluidic chips.[82] PDMS is highly permeable to gasses and has frequently been employed in production of cell-microfluidic applications.[82] Cells-on-a-chip devices which form μlung microfluidic support systems have great potential to expedite early stages of drug discovery or drug target analysis. Design and execution of microfluidic supported lung tissue combined with analysis of key disease biomarkers will also allow for production of high-throughput systems. Cheap, easily replicated, and standardized testing systems for evaluating lung toxicity would help to minimize the morbidity and mortality associated with drug-induced respiratory problems. More than 380 medications are known to cause pulmonary toxicity and this number increases as new medications are developed.[83,84] Diagnosis of drug-induced toxicity in the lung is usually based on clinical findings which include problems with respiration. Few systems to examine human drug toxicity in the lung exist and the adverse reactions that do occur can involve the pulmonary parenchyma, the pleura, the bronchi, and the vascular system of the lung (endothelium). Production of lung-on-a-chips containing cells or tissues using cells from one or, potentially, all of these regions of the distal lung would help us to develop a better understanding of drug-induced lung toxicity and will allow us to screen medications for potential lung toxicity before human use. Design of microfluidic supported lung tissues which consider the need for systems that support analysis of key lung disease biomarkers will also allow for production of

Table 2 Review of currently available upper and lower respiratory tract models

Author and Year Published	Description of Engineered Lung Model	Type of Model	Cell Source	Scaffold	Platform Systems for Tissue Culture	Final Cell Type Produced
Lwebuga-Mukasam[77]	Model used to study the modulating effect of the lung basement membrane on the morphology and function of type II pneumocytes.	Physiologic	Primary rat type II pneumocytes	Human lung acellular alveolar fragments	48-well tissue culture plates	AEC II (lamellar bodies)
Blau[5]	Development of alveolar-like structures (ALS) with central lumens. Model used to study the effects of a reconstituted basement membrane on fetal cell differentiation and long-term culture of pneumocytes.	Developmental, physiologic	Fetal rabbit cells from 29-day gestation	Engelbreth-Holm-Swarm (EHS) tumor membrane thick and thin gels	24-well culture plates	AEC II (lamellar bodies) Cells with microvilli facing central cavities
Sugihara[85]	Model used to study type II pneumocyte differentiation on a three-dimensional (3D) matrix and pulmonary disorders affecting alveoli.	Developmental, physiologic, pathologic	Primary rat type II pneumocytes from 21 - to 23-day-old rats	Collagen gel matrix	12-well tissue culture plates	AEC II
Chinoy[56]	Formation of alveolar-like structures	Developmental, physiologic	Fetal rabbit type II pneumocytes 22-day gestation	Engelbreth-Holm-Swarm (EHS) tumor membrane or Matrigel	24-well tissue culture plates	AEC II
Pugin[46]	Development of an *in vitro* ''plastic lung'' model with the ability to perform cyclic pressure-stretching of cells in culture. Model used to study the inflammatory response of a variety of lung cells including alveolar macrophages (AM) during mechanical ventilation-induced inflammation.	Physiologic, pathologic	A459 cells, EA.hy926 endothelial cells, human bronchial BET-1 A cells, human primary lung fibroblasts, human AM isolated from lavage of lungs with cancer, human monocyte-derived macrophages (MDMs) from peripheral blood, nonadherent promonocytic human THP-1 cells		Plastic lung made from transparent Plexiglas with a bottom chamber containing double 6-well plates. Bottom of wells contain Bioflex Silastic membranes	AEC II, endothelial cells, fibroblasts, bronchial epithelial cells AM (main source of inflammatory mediators—TNF-α, IL-8, IL-6, and matrix metalloproteinase-9)
Chakir[86]	Model of engineered human bronchial mucosa (EHBM) in air–liquid interface used to study mechanisms of inflammation, airway repair, and cellular interactions in asthma.	Physiologic, pathologic	Human bronchial epithelial cells and fibroblasts isolated from bronchial biopsy specimens of asthmatic and normal subjects. T lymphocytes isolated from the peripheral blood of asthmatic patients	Human fibroblasts incorporated into a collagen gel matrix	Petri dishes (35-mm diameter) containing an anchorage	EHBM with normal cells presented a pseudostratified ciliated epithelium with the presence of mucus secretory cells. Percentage of IL-5^+ lymphocytes was significantly higher in EHBM with asthmatic cells.

(continued)

Table 2 Continued

Author and Year Published	Description of Engineered Lung Model	Type of Model	Cell Source	Scaffold	Platform Systems for Tissue Culture	Final Cell Type Produced
Hermanns[47]	Co-culture system of human distal lung. Model used to study the alveolar–capillary barrier in the pathogenesis and recovery from acute lung injury.	Physiologic, pathologic	Primary human pulmonary microvascular endothelial cells (HPMEC) isolated from normal portions of lung specimens from patients who underwent lobectomies for early stage lung cancer. Human lung adenocarcinoma cell lines, A549 and NCI H441.		24-Transwell plates with a collagen type I coated filter	AEC II (TTF-1, SP-A, SP-B, SP-C, SP-D, E-cadherin, lamellar bodies) HPMEC (CD 31, VE-cadherin)
Paquette[87]	Production of bronchial equivalents (BE). Model used to study mechanisms involved in asthma.	Physiologic, pathologic	Primary human bronchial epithelial cells (HBEC) and human bronchial fibroblastic cells (HBFC) isolated from biopsies of normal and asthmatic lungs.	Mesenchymal layer composed of type I collagen gel with a HBFC suspension.	Petri dishes (35-mm diameter) containing peripheral anchorage (sterile ring of Whatman paper) and an internal elevated support	HBEC (Keratin, Gelatinase A MMP-2, Gelatinase B MMP-9) HBFC (vimentin) Numerous cilia in HBEC of normal lungs. Sparsely distributed cilia in HBEC from asthmatic lungs.
Matrosovich[88]	*In vitro* cell culture models of human airway epithelium. Model used to study cellular tropism of human and avian influenza viruses.	Pathologic	Primary human epithelial cells from tracheal/bronchial and nasal tissues.		Transwell culture plates	Nonciliated human tracheal epithelial cells (2-6-linked sialic acid receptors) Ciliated cells (2-3-linked sialic acid receptors) Secretory cells (identified by Alcian blue-periodic acid Schiff staining)
Chen[56]	Formation of lung histotypic alveolar-like structures. Model used to facilitate the study of strategies for preparing collagen-glycosaminoglycan (GAG) scaffolds for the regeneration of lung tissue.	Physiologic	Primary fetal lung cells from rats 16 and 19 days gestation.	Disk-like samples of type I collagen-(GAG) sheets	Agarose-coated 12-well tissue culture plates	AEC II Pseudo-stratified ciliated columnar epithelial cells 19-day cells surrounding alveolar-like structures expressed alpha smooth muscle actin

(continued)

Table 2 Continued

Author and Year Published	Description of Engineered Lung Model	Type of Model	Cell Source	Scaffold	Platform Systems for Tissue Culture	Final Cell Type Produced
						and were able to contract.
Coraux[61]	Culture model of airway epithelium in an air–liquid interface from differentiated murine embryonic stem (ES) cells. Model used to study methods of cell therapy to reconstitute airway epithelium in airway diseases, such as bronchopulmonary dysplasia, cystic fibrosis, or bronchiolitis obliterans.	Developmental, physiologic	Undifferentiated mouse ES cell line CGR8		Petri dishes: type I collagen-coated, gelatin-coated, type IV collagen-coated, or type VI collagen-coated. Millicell-HA porous membranes placed on dishes.	Basal cells (GS-I-B4) Ciliated cells (tubulin β) Intermediate cells Nonciliated Clara cells (CC10, SP-D, abundant rough endoplasmic reticulum, numerous mitochondria and electron-dense secretory granules)
Choe[72]	Model of human bronchial mucosa cultured at an air–liquid interface that mimics anatomical and functional features of the airway wall. Model used to study airway remodeling, transepithelial transport, and inflammatory cell interactions.	Physiologic, pathologic, toxicological	Normal human bronchial epithelial cells (NHBEs) Human fetal lung fibroblasts (HLFs)	Type 1 collagen gel	6-well transwell plates with porous polymeric wells	Ciliated cells Mucus secreting cells
Cortiella[62]	Alveolar tissue growth *in vitro* and *in vivo* from differentiated ovine somatic lung progenitor cells (SLPCs) capable of generating lung tissue. Model used to study the potential of progenitor stem cells and scaffold-based methods in the generation of lung tissue.	Developmental, physiologic	Primary ovine SLPCs isolated from lung tissue	Polyglycolic acid (PGA) matrix Pluronic F-127 (PF-127) matrix	175 mL flasks	Clara cells (CC10) AEC II (SP-C, Cytokeratin)
Mondrinos[57]	Pulmonary tissue constructs that mimic distal lung architecture by formation of alveolar forming units (AFU) and branching morphogenesis. Model used to study the generation of distal pulmonary tissue for replacing diseased lung tissue such as in neonatal pulmonary hypoplasia.	Developmental, physiological, pathological	Primary murine embryonic day 18 fetal pulmonary cells (FPC)	Porous foams and nanofibrous matrices of Matrigel hydrogel, poly-lactic-*co*-glycolic acid (PLGA), poly-l-lactic-acid (PLLA)	55 mL rotating wall vessel bioreactor	AEC II (SP-C, lamellar bodies) Mesenchymal cells (vimentin) Mesenchymal-derived morphogenic inducer of the epithelium (FGF 10), epithelial morphogenetic receptor (FGFr2)
Mondrinos[58]	Model of fetal distal lung tissue in which an epithelial–endothelial interface is observed. Model used to study lung	Developmental, physiological, pathological	Primary murine embryonic day 17.5 FPC	Type I collagen gel matrix	24-well culture plates	AEC II (pro-SP-C, cytokeratin) Endothelial cells (CD 31,

(continued)

Table 2 Continued

Author and Year Published	Description of Engineered Lung Model	Type of Model	Cell Source	Scaffold	Platform Systems for Tissue Culture	Final Cell Type Produced
	development and for methods of generating lung constructs for lung augmentation in pediatric pulmonary pathologies.					PECAM-1, VEGFR1, VEGFR2, isolectinB4) Mesenchymal cells (vimentin, tropoelastin) Epithelial–endothelial interfacing (FGF10/7/2)
Andrade[59]	Generation of porous structures that are similar to alveolar units. Model used to study the potential of cell- and scaffold-based techniques for lung regeneration.	Developmental, physiological	Rat fetal lung cells	Gelfoam sponge	Gelfoam implantation into rat lungs	AEC II (pro-SP-C) Clara cells (CCSP) Endothelial cells (von Willebrand factor) Infiltrating leukocytes (CD45)
Birkness[89]	Rounded cellular aggregates of human cells used as a model to study granuloma formation and cellular and immunological responses during *Mycobacterium tuberculosis* infection.	Pathologic	Peripheral blood mononuclear cells (PBMCs) isolated from whole blood of healthy donors.		24-well culture plates	Macrophages (CD68) T lymphocytes (CD3)
Zani[63]	*In vivo* airway injury model using collagen matrices engrafted with human epithelial and endothelial cells. Model used to study airway injury and repair.	Physiologic, pathologic	Human bronchial epithelial (EP) cells, human aortic endothelial cells (EC) HUVECs Normal human lung fibroblast cell line (NHLF)	Tissue culture polystyrene (TCPS) coated with Gelfoam	15-mL polypropylene tubes 48-well plates Matrices implanted into rabbit tracheas	Cuboidal basal cells Squamous mucus cells EP and EC cells (sICAM-1 production, production of pro-inflammatory cytokines)
Cortiella[3]	Generation of 3D upper and lower respiratory tract lung tissue using differentiated murine embryonic stem cells (mESC) on a whole natural lung matrix. Model used to study the effects of natural lung matrix on ESC differentiation into lung-specific lineages.	Developmental, physiologic	mESC	Whole acellular (AC) rat lung matrix	50 mL rotary bioreactor	Ciliated epithelial cells (cytokeratin-18) Clara cells (CC10) AEC II (pro-SP-C) Developing epithelium (TTF-1) Endothelial cells (CD31, PECAM-1) Smooth muscle cells (α-SMA)
Huh[48]	Biomimetic microsystem with an air–liquid interface that reconstitutes the alveolar–capillary interface of the	Physiologic, pathologic, toxicological	Cell line of human microvascular endothelial cells, HUVEC,	Microporous PDMS membranes coated	Microfluidic device with microchannels that is	AEC II (lamellar bodies surfactant production)

(continued)

Table 2 Continued

Author and Year Published	Description of Engineered Lung Model	Type of Model	Cell Source	Scaffold	Platform Systems for Tissue Culture	Final Cell Type Produced
	lung. Microengineered system used as a model to study cellular interactions and responses to nanoparticles. Systems may also be used as models for high-throughput screening of drugs, toxins, or pathogens.		human alveolar epithelial cells (NCI H441), A549, E10 (an immortalized, nontumorigenic cell line derived from alveolar type II pneumocytes), human dendritic cells isolated from whole blood of healthy donors	with collagen gel or fibronectin	integrated with computer-controlled vacuum to produce cyclic stretching	Endothelial cells (ICAM-1, VE-cadherin)
Miller[73]	Development of a human lung cylindrical-shaped bronchiole model in an air interface. Model used to study mechanisms of airway remodeling	Physiologic	Human primary normal lung fibroblasts (CC2512) Human airway smooth muscle cells (CC2576) Human small airway epithelial cells (CC2547)	Type I collagen gel matrix with embedded human lung fibroblasts	Bioreactor that contains a polytetrafluoroethylene (PTFE) mold unit	Human lung fibroblasts (β-tubulin) Human small airway epithelial cells (cytokeratin-18, collagen IV, mucin, K-19, production of cilia) Smooth muscle cells (α-SMA, smooth muscle myosin heavy chain, vimentin)
Ott[49]	*In vitro* formation of lung tissue constructs that contain epithelial and endothelial lung tissue. Regenerated lung constructs were transplanted into orthotopic position and assessed for *in vivo* function. Model used to study methods of lung regeneration.	Developmental, physiologic	A549 Rat fetal lung cells HUVEC	Whole acellular rat lung matrix	Bioreactor	AEC II (pro-SP-C, SP-A, Ttf1) Caveolin-1 AEC I (T1-α) Fibroblasts (vimentin)
Petersen[75]	Engineered lungs that display many microarchitectural features of native lung and that function in gas exchange for short periods of time when implanted into rats. Model used to study if lung tissue can be regenerated *in vitro* using decellularized tissues as scaffolds.	Developmental, physiological	Mixed populations of neonatal rat lung epithelial cells Microvascular lung endothelial cells	Decellularized rat lung	Bioreactor	Ciliated columnar epithelial cells Clara cells (CCSP) AEC I (AQP5) AEC II (pro-SP-B, pro-SP-C) Endothelial cells (CD31)
Price[60]	Development of a bioreactor system to produce natural lung matrices from decellularized tissues. Model used to study components of a	Developmental, physiologic	Mice embryonic day 7 fetal lung cells	Decellularized mice lungs	Culture flask filter cap bioreactor system	AEC II (pro-SP-C) AEC I (AQP5) Endothelial cells (CD31) Fibroblasts (vimentin)

(continued)

Table 2 Continued

Author and Year Published	Description of Engineered Lung Model	Type of Model	Cell Source	Scaffold	Platform Systems for Tissue Culture	Final Cell Type Produced
	decellularized lung matrix and its ability to support lung tissue development.					
Nguyen[90]	Generation of an organotypic model of the human airway mucosa. Model used to study the influence of the tissue microenvironment on regulating dendritic cell (DC) functions during homeostasis or an inflammatory response.	Physiologic	Human lung fibroblast cell line, MRC-5 derived from normal lung tissue of a 14-week-old male fetus. 16HBE, an immortalized human bronchial epithelial cell line. Human monocyte-derived DC isolated from whole blood.	Collagen gel matrix seeded with fibroblasts	6-well plates with 3.0-μm transwell inserts	DC (DC-SIGN, positive for CD1a and negative for CD14)
Huh[5]	Development of a microfluidic device with air and fluid flow that mimics the alveolar–capillary interface of the human lung. Microfluidic device used as a model of pulmonary edema.	Physiologic, pathologic, toxicological	Human alveolar epithelial cell line NCI-H441. Cell line of human pulmonary microvascular endothelial cells.	Porous membranes coated with fibronectin	Microfluidic device with upper and lower microchannels	AEC II Microvascular endothelial cell junctional proteins (VE-cadherin, occludin)
Kloxin[50]	Cell culture platform in which the geometry and connectivity of the cellular microenvironment is controlled spatiotemporally. Model used to study how cellular interactions are affected by static or evolving environmental cues and how this modulates tissue development.	Physiologic	A549 cell line isolated from human lung adenocarcinoma. Primary AEC II isolated from rat distal lung tissue.	Hydrogel layers on photolabile, enzyme-labile base material	12-well culture plates	AEC II (pro-SP-C) AEC I (T1-α)
Patel[51]	Dynamic cell growth system to mimic the mechanical environment of the lung. Model used to study pneumocyte proliferation and oxidative and inflammatory response to multiwalled carbon nanotubes (MWCNT) in dynamic versus static growth conditions.	Physiologic, pathologic	A549 cell line that is type II epithelial-like in morphology and originates from a human lung adenocarcinoma.		6-well BioFlex plates with a Tension Plus 4000T system	AEC II
Booth[91]	Culture system of acellular human lung matrices from normal lungs and fibrotic lungs seeded with human cells to create lung constructs.	Physiologic, pathologic	Primary human lung fibroblasts were isolated.	Biopsy punch cylinders of decellularized lung matrices	24-well culture plates	Myofibroblasts (α-SMA, cellular fibronectin)

(continued)

Table 2 Continued

Author and Year Published	Description of Engineered Lung Model	Type of Model	Cell Source	Scaffold	Platform Systems for Tissue Culture	Final Cell Type Produced
	Model used to study how the extracellular matrix of normal and fibrotic lungs influences fibroblast phenotype.			from normal healthy lungs and from interstitial pulmonary fibrosis patients		
Bonvillain[92]	Development of a nonhuman primate lung model using decellularized Rhesus macaques lungs and mesenchymal stem cells. Model used to study the effects of decellularized lung matrix on cell attachment, elongation, and proliferation.	Developmental, physiologic	Rhesus primary bone marrow-derived mesenchymal stem cells (BMSC) and adipose-derived mesenchymal stem cells (ASC).	Lower lobes of acellular Rhesus macaque lungs with an agarose mixture as a vehicle for seeding cells	6-well plates	BMSC and ASC (assessment of proliferation; Ki67- and TUNEL-positive)
Horie[52]	3D co-culture assay of human lung cancer cells. Model used to study the tumor-promoting abilities of cancer-associated fibroblasts (CAFs) when compared to normal fibroblasts (NF)	Physiologic, pathologic	Human lung adenocarcinoma cell line A549 Primary human lung fibroblasts isolated-patient-matched CAFs and NFs from tumoral and nontumoral portions of resected lung tissue from lung cancer patients.	Type I collagen gel matrices	6-well culture plates	CAFs (α-SMA, enhanced collagen gel contraction) Both CAF and NF (vimentin, pan-keratin)
Nichols[45]	Development of lung tissue constructs using acellular pig and human lung matrices seeded with a variety of different cell types. Model used to support *in vitro* development of lung tissue using natural lung matrices.	Physiologic	Murine embryonic stem cells (mESC), human fetal lung cells (HFLC), pig bone marrow-derived mesenchymal stem cells (BMMSCs) and primary human alveolar epithelial type II cells (HAEC), which are predominantly AEC II.	0.5 cm^3 pieces of acellular porcine and human lungs, Matrigel, or Gelfoam	24-well culture plates	AEC II (pro-SP-C) AEC I (AQP5)
Mishra[53]	Development of an *ex vivo* lung cancer model using natural lung matrix with human cancer cells. Model forms tumor modules and is used to study progression of tumor growth.	Pathologic	Human alveolar basal epithelial cell line A549.	Decellularized rat lungs	Bioreactor	AEC II

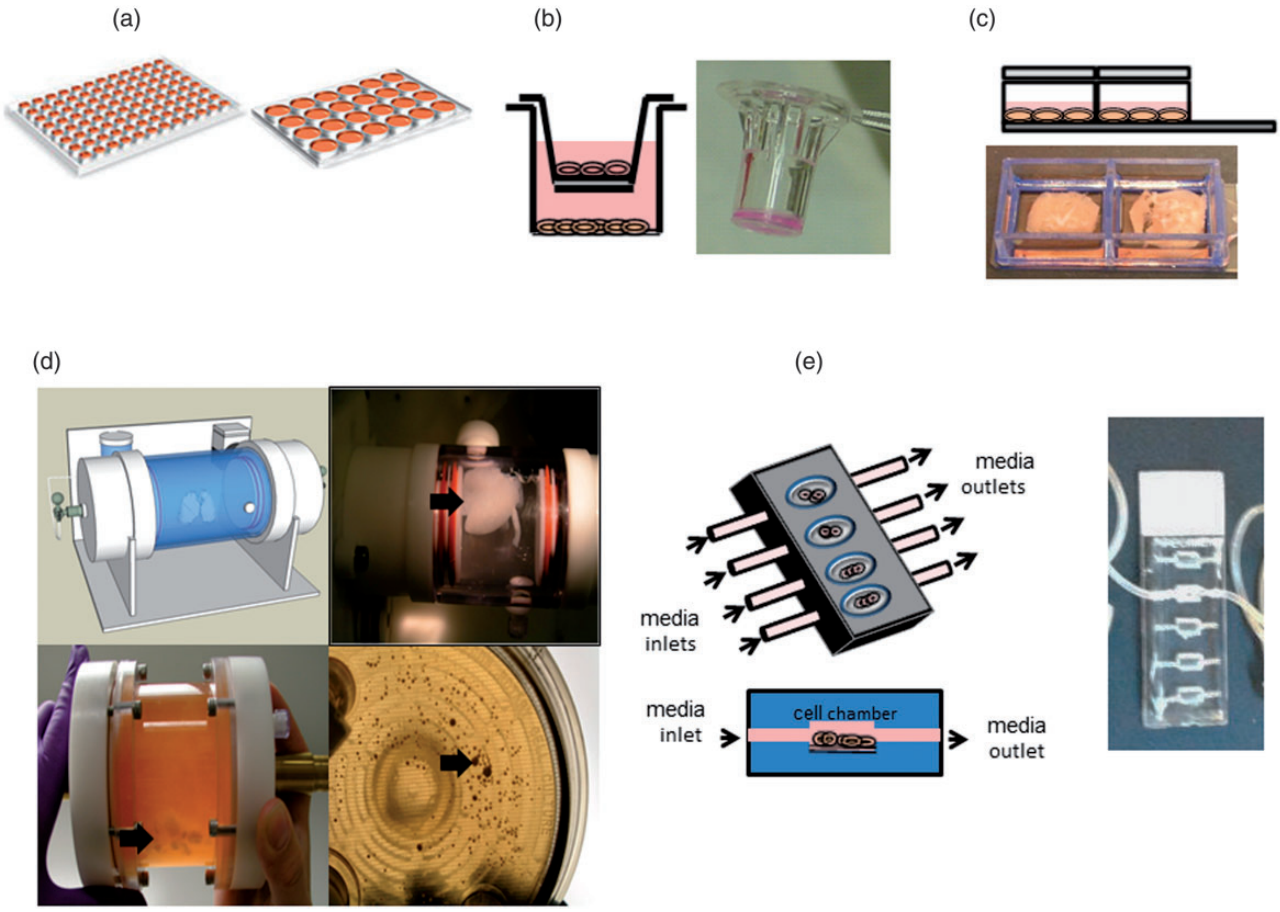

Figure 1 Platforms used in the development of 3D lung tissue models. (a) 12-, 24-, 96-well format plates. (b) Transwell type culture platform. (c) Slide chamber platform for support of imaging of 3D lung tissue. (d) Rotary bioreactor for culture of 3D lung constructs.[3] Black arrow points to either whole trachea–lung culture (top right) or aggregate cultures of alveolar type I and II cells (bottom right). (e) Diagram of a basic microfluidic system with media inlet and outlet ports and image of current chamber system produced by the authors for lung cell culture (unpublished data). (A color version of this figure is available in the online journal.)

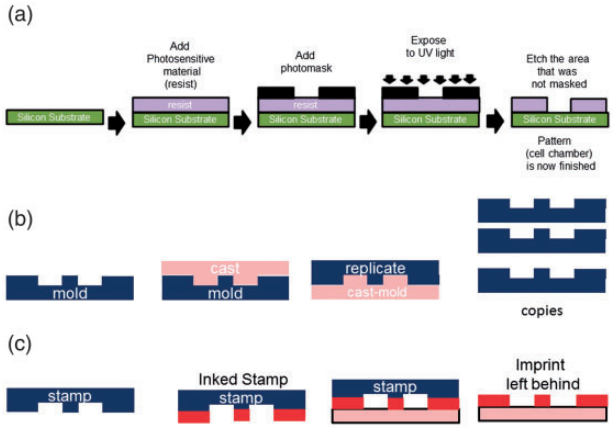

Figure 2 Methods for production of microfluidic supported cell culture systems. (a) Photolithography which uses light to transfer a pattern from a photomask to a light sensitive chemical resist, placed on a substrate. (b) Replica molding which creates many copies of a specific pattern or structure by creation of a mold and then a reverse mold to create copies. (c) Microcontact printing which is a form of soft lithography where patterns are transferred to a surface using a stamp. (A color version of this figure is available in the online journal.)

more useful high-throughput systems to examine lung diseases in the future.

The main problems associated with design and development of microfluidic support systems for 2D microfluidics culture are related to design of the platform and include control of tissue perfusion related to perfusion speed and force, need for bubble trapping, and determination of how cell responses will be analyzed. One of the motivations for use of microfluidic supported cell platforms is the automation of labor-intensive fluid transfer procedures. Media perfusion rates must be low enough (less than 1 mL/day) that fluid flow in the cell chamber does not interfere with cell or tissue responses or with immune cell migration. Bubble trapping may require the incorporation of bubble traps existing in the platform itself or in the media reservoir line. Release of small bubbles into the cell chamber alters cell responses and reduces the ability to image cells or collect standardized aliquots of culture supernatants. Determinations related to analysis of cell viability, cytokine production, or metabolite evaluation need to be dealt with during the design phase of platform development. HoC systems allow for production of high enough levels of

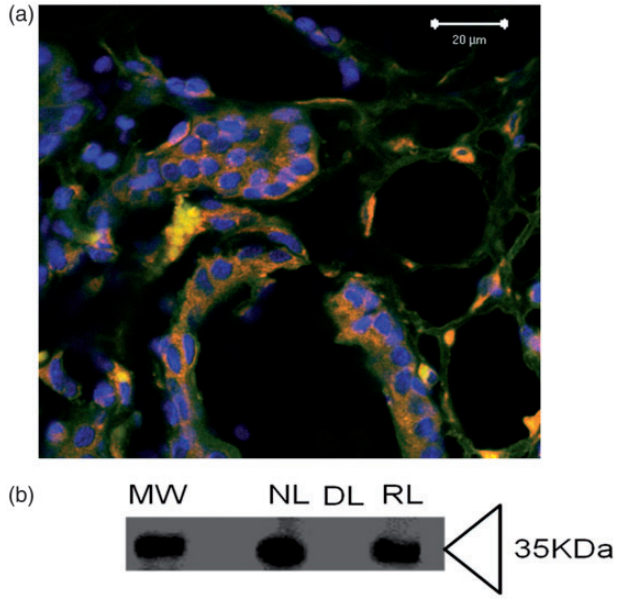

Figure 3 Production of lung-specific biomarkers by a distal lung human organ construct (HoC) system. HoC system (containing an estimated 6–9 million cells) with identification of lung protein markers by (a) immunocytochemistry for identification of surfactant protein-A (SP-A) or (b) immunoprecipitation of SP-A. The HoC was produced on whole trachea–lung scaffolds which were cultured in a rotary bioreactor for 21 days. (This is a revision of the original figure and is reprinted with permission from the authors). Blue nuclear stain is 4′,6′ diamino-2-phenylindole (DAPI). SP-A (red) is indicated by positive phycoerythrin (PE) staining. (A color version of this figure is available in the online journal.)[3]

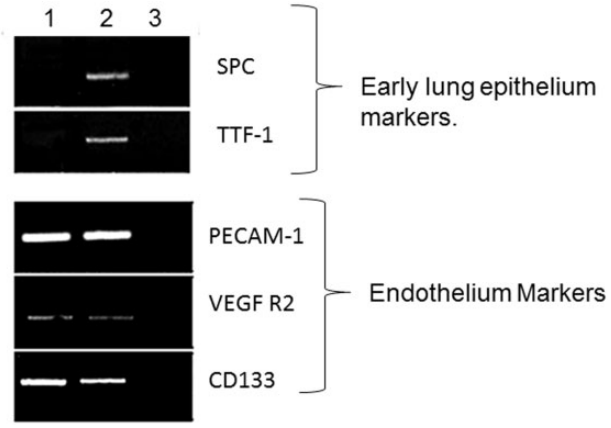

Figure 4 Expression of epithelial and endothelial marker genes from human μlung cultures cultures. Human μlung containing 1–1.5 million cells were evaluated using PCR for evaluation of development of lung epithelium and endothelium. (1) Spontaneously differentiated murine embryonic stem cells (mESC), (2) differentiated mESC enriched for potential to give rise to lung epithelium and grown on a lung acellular (AC) scaffold and AC scaffold alone. Presence of RNA for surfactant protein C, SP-C; TTF-1, thyroid transcription factor-1, TTF-1; Platelet endothelial cell adhesion molecule-1, PECAM-1; Vascular endothelial growth factor receptor-2,$VEGFR_2$ (Authors unpublished data) was examined.

proteins that immunostaining and standard techniques such as enzyme-linked immunosorbent assay (ELISA) or immuneprecipitation of proteins such as SP-A can be used to identify biological products (Figure 3). For analysis readouts that require microscopy special incubator, chambers housing specialized microscopes may need to be constructed.[93,94] Analysis systems that focus on biologic targets produced by chip experiments are more difficult to accomplish. Microfluidics systems handle microliter in microchannels 1–1000 μm in size[48] which severely limits the volume of harvested cell supernatants. Polymerase chain reaction (PCR) can be used to identify the presence of lung specific products such as surfactant proteins A, B, C, and D or thyroid transcription factor-1 (TTF-1) by lung progenitor cells or the presence of endothelial markers such as platelet endothelial cell adhesion molecule (PECAM-1), vascular endothelial growth factor (VEGFR), or CD133 when culturing endothelial cells (Figure 4). For small lung-on-a chip systems PCR analysis of cell products such as those mentioned earlier may not be possible. Specialized techniques such as real time (RT-qPCR)[96,97] or cycling probe technology have been designed as alternatives to PCR specifically for sample analysis related to microfluidic or chip experiments[98,99] and other micro-analytical methods such as gas-phase chromatography and capillary electrophoresis may also be used. Single-cell analysis strategies for gene expression, single-cell mRNA analysis, or single-cell DNA sequencing based on microfluidic technology have already been developed and can be coupled to cell-on-a-chip systems to allow for examination of molecular events related to cell responses.[100–102]

Evaluation and validation of model systems

Evaluation of engineered respiratory tissue models includes measurements of cell functionality and cell response. In order to successfully develop lung tissue models, evaluation of cell types, cell survival, and attachment of cells to scaffolds or generation of cell products is necessary to ensure the functionality of the model. For physiologic lung models, early lung products of epithelial cells have been used to indicate the ability of lung epithelial cells to function. Some of these products have included production of surfactant proteins A–D by type II AECs[3,45,47–50,57–60,62,75] and Clara cell protein-10 (CC10) generated by Clara cells.[3,61,62] In later developmental models of the lung produced using FLCs or ESCs, markers of cell differentiation included TTF-1[3] which is produced by immature epithelial cell types as well as surfactant protein-C, a type II AEC product of more mature cells.[3] Obviously for respiratory tissue mimics, production of mucin by cells in the trachea,[63,72,73,86] surfactant proteins by Clara or type II AEC cells,[45,47,59,75] or other lung specific biomarkers are indicators of successful tissue development. Respiratory tract toxicology models often use cell viability or induction of apoptosis as indicators of appropriate cell responses.[5,48,72] Pathogenesis and infectious disease models require an understanding of the disease to be modeled as well as the types of cells involved in a pathological response.[103–106] The ability to deconstruct a response using the fewest cell types required to elicit that response is what makes design and production of human engineered models both problematic and captivating. Once a disease model has been produced it must be standardized. Simple one- or two-cell based μlung models are fairly easy to standardize but

complex macro-physiological systems, HoC, which require large numbers of cells, many different cell types or formation of tissue in specific patterns such as endothelium and distal lung are much more difficult. Models that require a functional immune response are also difficult to construct and standardize. Addition of innate immune cells to model systems does not require consideration of human leukocyte antigen (HLA) tissue type but use of T and B lymphocytes in engineered tissue models may require development of immune tolerant cells or at least an HLA or tissue type half-match between the donor cells and the engineered tissue model. Validating production of lung lineage cell products or expression of specific lung associated membrane proteins or transcription factors using PCR, gel electrophoresis, or other methods is necessary especially when designing more advanced toxicology, pathogenesis, or infectious disease models of the lung. Tissue models must also be subjected to evaluation of precision as a test platform. Examination of intra-assay (within) and inter-assay (between) variability must be done for each model system once it has been established and shown to be reproducible and is the reason that plate culture experiments are usually done in triplicate with presentation of the data as a mean and standard deviation for each set of data. Intra-assay variation describes the variation of results within a data set obtained from one experiment. Inter-assay variation is the amount of variation between experiments done at different times. This is a good indicator of reproducibility of the model and how it will function over time. The reproducibility between assays should be monitored by the use of untreated controls. Analyzing controls along with experimental unknowns in each tissue model should give reliable evaluations and conclusions, although the experiments may have been conducted at different times.

Current perfused models of lung function

Microfluidic lung models currently described in the literature examine engineering principles (sheer stress, influence of pressure gradients, mechanical strain, and surfactant-induced airway tensions) rather than biological principles. Many of the microfluidic platforms for respiratory tract modeling that have been recently developed are designed to mimic the alveolar–capillary interface.[48,107] In order to recreate the epithelial and endothelial barrier, porous membranes coated with collagen gels are often placed between micro-channels. These collagen-coated membranes are also thought to provide an ECM-like three-dimensionality for the system but cells are cultured as monolayers within micro-channels.[48] To study the effect of mechanical ventilation on the epithelial cell barrier, human AECs lines (A549 and H441) were cultured on a multiphase microfluidic platform to mimic alveoli.[108] This microfluidic platform is referred to as a pressure chip that contains a top sealing panel and a base imaging panel, with each of these panels containing eight culture wells. Side access ports on the pressure chip are used as inlets and outlets for medium flow and air flow which allow air pressure to be applied. One of the interesting features of this pressure chip is that on the basolateral surface, medium is replenished at a continuous low flow and at the same time, on the apical surface the air flow maintains a steady rate.[108] This was also a key feature of the microfluidic platform designed by Huh *et al.*[48] Similar features are important to consider when designing macro- or micro-fluidic platforms for lung models that require an air–liquid interface to better resemble *in vivo* physiological conditions. The development of this pressure chip allows for studies of ventilator-induced lung injury (VILI) or other conditions where the lung is exposed to mechanical disruptions or aerodynamic sheer stress.[108] For this study, alveolar membrane integrity was measured as transepithelial electrical resistance (TEER) upon cell exposure to pressure of varying magnitudes, and measurements of TEER were taken at 24-h intervals.[108] Preliminary results indicated a dose-dependent response where cells exposed to higher air-pressure magnitudes showed a net decrease in TEER. Disruptions of cell layers were observed during pressure application although cells seemed to recover in the postapplication period and minimal cell death was observed.[108]

Although the design of this pressure chip allows it to be used in various applications and may provide insights about cellular responses and cell–cell interactions when exposed to different stresses, there are limitations to the use of this platform. One of these limitations is that results obtained from this pressure chip are not necessarily comparable to human physiological responses even though human cells are used because cells are cultured on the pressure chip as monolayers or multilayers of stacked cells that greatly differ from their organization in lung tissue. Cellular behavior and responses are altered by this change in composition and results may be misleading when compared to their responses *in vivo* where the structural microenvironment influences reactions.

The mechanics of fluid flow in the pulmonary system is of great importance in the design of models that better recreate interfacial flows that happen when injury or disease causes liquid obstructions within the airways.[109] An example of this is acute lung injury in which disruption of the alveolar–capillary junctions leads to increased permeability allowing the entry of fluid and inflammatory mediators that will result in pulmonary edema and prevent breathing. Understanding the effect of liquid obstructions or surface tension stresses on airway closure and reopening is an integral part of biofluid interactions between the airways and vasculature of the lungs. The viscoelastic properties of surfactant and mucus must also be considered when comparing pathological conditions with normal physiology in the airways.[109] Current models of pulmonary airways containing epithelium and endothelium are simplified models consisting of single airways, collagen gel-based systems, or microfluidic systems that try to recreate small components of the alveolar–capillary interface.[48,72,73] It is important to understand that cellular responses within simplified systems or cell monolayers that lie flat on micro-channels or other surfaces will be very different when compared to their responses within the ECM of the tissues. Although these models have provided valuable insights about pathologic alterations to the lungs, the

structure and design of these models is very different from the 3D architecture of the human airways where responses are interdependent within regions of the lungs. Development of more complex models that contain distal lung regions with numerous alveoli interconnected with bronchial airways and blood vessels is necessary to reproduce the dynamic *in vivo* setting in the human lungs. Models that have a more complete lung ultrastructure will be essential in understanding how mechanical stresses and fluid flows affect cellular responses and the integrity of cellular membranes in a more realistic macroenvironment. The use of the natural lung ECM for development of more complex macromolecular models or possibly whole-lung lobe models is a suitable method since it already contains the necessary 3D structure, mechanical properties, chemical composition, and structural organization of native lung.[110]

2D and 3D physiologic models of trachea or upper respiratory tract

We have attempted to provide a broad overview of current upper and lower respiratory tract models and these are presented in Table 2. We selected studies based on (1) cell type used, (2) scaffold material, (3) platform, (4) goal of the study (development of physiologic tissue, evaluation of toxicity, use in pathogenesis studies), or (5) novelty of platform design or goal of study. An early but well-designed pathologic 3D model of upper airway was engineered from human bronchial mucosa grown on a collagen gel scaffold seeded with primary cells derived from normal and asthmatic lung tissues cultured in an air–liquid interface.[86] In this study, human bronchial fibroblasts from normal and asthmatic donors were incorporated into a collagen gel. Bronchial epithelial cells were seeded over this gel and then cultured in an air–liquid interface in the presence or the absence of T lymphocytes. Small biopsy specimens from these models of engineered mucosa were taken for structural and ultrastructural analysis, and T lymphocytes were harvested and used to localize interleukin-5 (IL-5). Histologic analysis showed that engineered mucosa with normal bronchial cells presented a pseudostratified ciliated epithelium with the presence of mucus secretory cells. Electron microscopy analysis confirmed these histologic results. These features were comparable with those observed in normal bronchial tissues. However, in engineered mucosa from asthmatic subjects, the tissue structure was disorganized, particularly the epithelial cell arrangement. The percentage of IL-5 positive lymphocytes was significantly ($P = .03$) higher in engineered bronchial mucosa from asthmatic subjects ($87\% \pm 2\%$) compared with mucosa from normal volunteers ($2\% \pm 0.3\%$).[86] Another physiologic model of bronchi was developed from mESC seeded onto type I collagen coated dishes.[61] This culture model allowed for derivation of the principal cell types composing the airway epithelium (basal cells, Clara cells, and ciliated airway epithelial cells) from mESCs. The cells in this culture model organized themselves to give rise to fully mature epithelial airway tissue containing ciliated airway epithelium and Clara cells producing CC10 as well as SP-D. Later 3D models of human bronchial mucosa were generated using porous polymeric wells and a collagen gel scaffold[72] or implants of the bronchial epithelium and endothelium using Gelfoam collagen matrices as scaffolds.[73] Models of human airway have been used to study mechanisms of airway remodeling using a cylindrical--shaped bronchiole model in an air interface seeded with normal lung fibroblasts, human airway smooth muscle cells, and human small airway epithelial cells.[73] One complex organotypic model of airway mucosa was used to evaluate the influence of the tissue microenvironment on regulating dendritic cell (DC) functions during homeostasis or an inflammatory response.[90] This model contained human fibroblasts, bronchial epithelial cells, and human peripheral blood monocyte-derived DC.

The respiratory tract models listed earlier were not produced using microfluidic support platforms and all required a great deal of manual manipulation for addition of media, removal of waste, or for sample harvesting. All of these models provided critical information regarding lung cell or tissue responses, but survival of cells in these types of *in vitro* models has been limited due to lack of simple perfusion systems for media exchange and waste removal which are currently under development.

Current 3D lung models or HoC

Early lung system models (Table 2) functioned mainly as physiologic models and provided for examination of basic components of AEC function when AECs were cultured on natural lung AC scaffold,[77] EHS tumor membrane,[54] collagen,[55,85] or Matrigel.[55] The goal of these early studies was to maintain primary type II AECs *in vitro*. One early model was designed to study the inflammatory response of a variety of lung cells including alveolar macrophages during mechanical ventilation-induced inflammation.[46] This model, based on use of human transformed cell lines and primary human monocyte–macrophages, provided basic information related to the influence of stretch on immune and lung cell responses.

Attempts were made later to engineer alveolar–capillary junctions[47] or alveolar-like structures using rat FLCs seeded onto glycosaminoglycan scaffolds.[56] SLPC seeded onto PGA and PF-127 were shown to develop into lung tissue.[62] *In vitro* differentiation of a mixture of ovine SLPCs into pulmonary epithelium on PGA or PF-127 scaffolds with expression of CC10, cytokeratin, and SP-C was validated by western blot. Scanning electron microscopy (SEM) of the engineered tissue demonstrated organization of the cells into identifiable pulmonary structures morphologically similar to alveoli.[62] Other attempts to produce alveolar like structures *in vitro* include work by Mondrinos *et al*.[57] and Andrade *et al*.[59] In these simple models of the lung, fetal rat cells were seeded onto Gelfoam,[59] Matrigel, PLGA, and PLLA scaffolds.[57] During this period of time cell–scaffold constructs were made from a variety of source materials. Often alveolar development was limited due to poor design of scaffold materials that did not meet the specific needs of lung epithelial cells.

Use of models to examine stem cell responses, cell differentiation, or lung development

One of the first lung developmental models was produced from primary isolates of fetal pulmonary cells grown in collagen gel scaffold.[58] This system was used to test the differential effects of fibroblast growth factor (FGF)-2, FGF-7, and FGF-10 on distal lung morphogenesis. Results showed that FGF-2/7/10 induced robust budding of the epithelial structures and supported formation of a uniform endothelial network. A series of studies using whole-trachea lungs produced on AC natural lung showed that the scaffold supported growth and differentiation of rat FLCs,[49] rat neonatal lung cells,[75] and mouse embryonic lung cells[60] as well as formation of lung epithelial cells and, in some instances, endothelial cells[3,60,75] and primary AECs.[45]

We are just beginning to understand the influence of lung ECM on the differentiation of stem or progenitor cells and on subsequent tissue formation. Studies to examine this role have been limited although the field of tensegrity-based mechano-sensing suggests that (1) regional variation of ECM remodeling that occurs during embryogenesis leads to local differences in ECM structure and mechanics, (2) changes in matrix compliance (e.g. increased stiffness when the basement membrane is stretched) alter mechanical forces across membrane receptors that mediate cell–ECM adhesion, and (3) altering the level of forces that are transmitted to the internal cytoskeleton will produce cell structural changes and alter intracellular biochemistry, thereby causing cells to switch between growth, differentiation, and apoptosis.[111] In the respiratory tract the regional variability that occurs in ECM in both composition and stiffness as one progresses from the trachea to the bronchi and bronchioles and then to distal lung is extensive. One of the first reports regarding the influence of ECM on ESC differentiation into lung epithelial and endothelial lineages examined the efficiency of differentiation after allowing mESCs to attach to individual components of ECM. In these studies ECM proteins, such as collagen I, laminin, and fibronectin, were shown to induce production of type II AEC from mESC cultured in 2D or 3D.[112] Efficiency of differentiation of mESCs into lung lineage phenotypes was measured by expression of SP-C-eGFP in cells using microscopy and PCR. Production of SP-C and -A by type II AEC and aquaporin-5 (AQP5) by type I AEC were enhanced by the presence of laminin. Similar results were found when mESCs were cultured on whole AC rat lung scaffold in order to examine the role of ECM on site-specific differentiation of stem cells.[3] Efficiency of differentiation in this model was measured by evaluation of CD31, cytokeratin-18, and pro-SP-C expression, which was shown to be increased by mESCs cultured on AC lung compared to commercially available matrices Gelfoam, collagen I, or Matrigel. Production of organized lung tissue as well as significant production of surfactant proteins A and C was only seen for mESCs cultured on AC lung and not on any of the other matrices used.[3]

Changes in ECM structure and composition have the ability to influence cell adhesion and provide critical cues that orchestrate tissue formation and induce cell responses via signaling through integrin-mediated pathways. Cells directly sense the rigidity of the local site they are engrafting to during and studies have examined the relative ECM stiffness at specific sites in the respiratory tract. Atomic force microscopy (AFM) and SEM studies examined the local stiffness of AC lung scaffold for five different sites: alveolar septa, alveolar junctions, pleura, and vessels' tunica intima and tunica adventitia. The local stiffness of the matrix materials significantly depended on the site within the matrix ($p < 0.001$), ranging from ~15 kPa at the alveolar septum to ~60 kPa at the tunica intima.[113] Figure 5 shows a whole AC rat lung, the site of AFM probe placement, and an SEM of the scaffold in the region of the alveolar septum and potential AEC attachment. These stiffness differences must be considered when developing microfabricated chambers or selecting scaffolds for respiratory tract modeling. Other reports also support the concept that organ-specific stroma or ECM may even be required for proper site-specific differentiation and organization of lung tissues.[3,114] A comparison between liver- and lung-derived AC scaffolds indicated that liver-derived scaffolds maintained the differentiation state of primary hepatocytes while lung-derived scaffolds allowed for both induction of lung lineage and maintenance of site-specific development

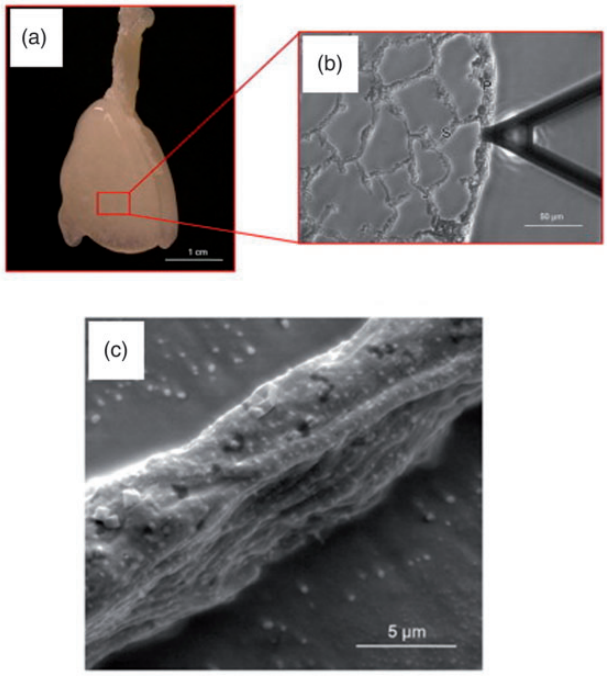

Figure 5 Components of acellular scaffolds which influence cell attachment and responses. How local micromechanical properties such as matrix stiffness and elasticity of decellularized lung scaffolds measured using atomic force microscopy.[115] (a) Decellularized whole rat lung, (b) AFM mechanical probe on distal lung portion of the scaffold showing alveolar septum, (c) scanning electron micrograph (SEM) of alveolar septum that was imaged using atomic force microscopy (AFM). (This is a revision of the original figure and is reprinted with permission from the authors). The micromechanical properties include the stiffness and elasticity of decellularized lung tissue. Different regions of the lungs, including the pleura, alveolar wall segment, and alveolar junction are probed by an AFM cantilever. (A color version of this figure is available in the online journal.)

of AE type II cells.[114] Recently, a well-based cell culture platform was developed that enables control of the geometry and connectivity of cellular microenvironments spatiotemporally. The base material is a hydrogel comprised of photo-labile and enzyme-labile crosslinks and pendant cell adhesion sequences, enabling spatially specific, *in situ* patterning with light and cell-dictated microenvironment remodeling through enzyme secretion.[50] Arrays of culture wells of varying shape and size were patterned into the hydrogel surface using photolithography. The geometry of these devices was subsequently modified through sequential patterning, while changes in cell geometry and connectivity were examined.[50] This type of *in vitro* system allows for dynamic evaluation of the influence of physical cues on tissue morphogenesis. The effect of well shape and size on lung epithelial cell differentiation (i.e. primary mouse type II AECs) was assessed using this model.[50] Shapes inspired by lung alveoli were produced on the hydrogel surfaces. Type II AECs were then seeded within the well-based arrays and encapsulated by the addition of a top hydrogel layer.[50] Cell differentiation in response to specific geometries was characterized over 7 days of culture with immunocytochemistry evaluation of lung lineages showing production of SP-C by type II AEC, proliferation and oxidative and inflammatory responses to multiwalled carbon nanotubes in dynamic versus static growth conditions.[51] Models have even been developed to study how the ECM of normal and fibrotic lungs influences fibroblast phenotype by using biopsy punch cylinders of decellularized lung matrices from normal healthy lungs and from interstitial pulmonary fibrosis patients.[91] Recent studies suggest that soft-lithography printing techniques that deposit appropriate cell matrix materials in systems supporting 2D culture of cells can mimic tissue-specific differentiation similar to that seen in 3D cultures.[116–118]

Physical forces also play an important role in influencing and regulating lung cell function and response and sensing of ECM–cell interactions influences cell responses. The lung is continually subjected to the complex physical forces produced by breathing and the pulmonary force of blood flow.[119] Breathing movements can be observed in the human fetus using sonography as early as 10 weeks of gestation.[119] Adhesion of cells to ECM is a critical regulator of cell function and integrin signaling plays a major role in cell signaling.[120–122] We also know that VILI and the physical forces exerted on lung cells can cause damage to the lung tissue.[123] Mechanotransduction induces a wide array of cellular responses and DNA microarrays of lung AEC subjected to culture platforms that evaluate stretch exhibit upregulation of genes involved in amino acid transport, growth factor receptors, and signaling molecules such as integrins.[124,125] Microfluidic platforms that provide for analysis of cell stretch have been produced which examine the influence of cell stretching on cellular responses[48,126–128] and tissue culture plates that allow for evaluation of stretch are currently commercially available from a number of sources.

Current lung pathology and infectious disease models

Identifying new therapeutic targets for lung disease relies on our basic understanding of the pathogenesis of various lung diseases. Recreating pathology can be challenging but important in order to isolate key players in the pathogenesis of a specific disease. Although *in vitro* models utilizing human tissue have been developed for certain pathologies such as lung cancer and pneumoconiosis, animal models or human pathology specimens have, so far, provided the basis for our understanding of human lung disease pathogenesis. Differences in genetics, immune response, metabolism, and anatomical structure make animals a less than perfect platform for studying human disease. A list of human lung diseases, the pathogenesis of the disease, the current animal models and, where appropriate, the *in vitro* lung tissue models used to mimic each disease are listed in Table 3. Emerging lung models using human cells and tissues could provide illuminating perspectives in lung disease pathogenesis and yet few systems have been produced. From a clinical perspective, it is essential to build accurate pathological models of lung disease to develop new targeted therapies. Some of the major categories of lung disease with pathologies that either have been or could be modeled include pulmonary edema, DAD, emphysema, sarcoidosis, bronchiolitis obliterans (BO), bronchiectasis, chronic interstitial lung disease, pneumoconiosis, pulmonary hypertension, and cancer. Table 3 contains a list of lung diseases, the pathology to be modeled for each disease, animal models used to approximate each disease, and *in vitro* model systems where they exist.

Microchip models of pulmonary edema

Most models of pulmonary edema have been designed to examine the development of edema in relation to microvascular injury and subsequent vascular leakage into the alveolar space and interstitium. A common approach to induce vascular leakage is the intravascular administration of interleukin-2 (IL-2) in *in vivo* animal models. One such animal study injected human recombinant IL-2 intravenously into rabbits to induce microvascular injury. The histological specimens of rabbit lung tissue closely mirrored human pathology of vascular leakage, cell damage, and pulmonary edema. The lung tissue showed separation of endothelial cells from the basement membrane, interstitial edema, and migration of lymphocytes into the interstitium.[129] Injecting IL-2 in animals provides a response similar to humans but is an imperfect model. Immune responses and signals developed differently in animals versus humans due to evolutionary pressures in individual biological niches.[130] Therefore, it is possible to induce pulmonary edema in animals using similar immune mechanisms in humans, but it is impossible to piece together an accurate model of pathogenesis. Unlike *in vitro* studies, factors such as production of and influence of an individual cytokine or chemokine or even specific responses of selected groups of immune cells are not easily determined *in vivo*. Therefore,

Table 3 Major categories of lung disease, cause, pathology modeled, animal models used, *in vitro* models available, and cell types necessary for model development

Major categories of lung disease	Causes	Pathology to be modeled	Animal model	*In vitro* model	Cells needed for model
Pulmonary edema	Hemodynamic or microvasculature injury	*Hemodynamic*: engorged alveolar capillaries, intra-alveolar exudates; in long-term cases induces hemosiderin macrophages and interstitial fibrosis. *Microvascular Injury*: damage to endothelium or alveolar epithelium, leakage of fluid and proteins into alveolar space.	*Hemodynamic:* Induction of heart failure through ligation of mice aorta results in hemodynamic pulmonary edema[131] *Microvascular injury*: IV injection of IL-2 or LPS induces microvascular injury in murine models[132] *Rat*-injected fluid solution into rat trachea and used negative pressure to ventilate rats while anesthetized to measure alveolar clearance[133] *Rabbit*: IV injectionion of human recombinant IL-2 into rabbits induced microvascular injury and leakage. Lungs showed a separation of endothelial cells from the basement membrane, interstitial edema, and migration of lymphocytes into interstitium[129]	*Microfluidics*: IL-2 administration through endothelial compartment caused leakage across endothelial lining into air-filled AEC I lined space. Alveolar–capillary leakage was enhanced by negative pressure breathing motions on either side of alveolar compartment[5]	Endothelial, AEC I
Diffuse alveolar damage (DAD)4	Infection, physical injury, chemical injury, hypersensitivity reactions	Damage to endothelium and epithelium, increased alveolar–capillary permeability, hyaline membrane, epithelial type II proliferation, neutrophil infiltrate, elevated pro-inflammatory mediators, eventual intra-alveolar fibrosis	See Matute-Bello *et al* 2008 Review, Table 4 for a complete list[130] *LPS:* IV injection of LPS is followed by a neutrophilic inflammatory response. There is limited alveolar–capillary permeability in this model, although it has been used as a model for pulmonary edema. *Hyperoxemia*: Hyperoxemia in animals induces a neutrophilic response, AEC II proliferation, and fibrous scarring. However, in humans hyperoxemia doesn't induce DAD. *Bleomycin*: Exposure to IT bleomycin causes acute inflammatory injury followed by reversible fibrosis, but does not elicit hyaline membranes formation or a neutrophilic response.	None	AEC I, AEC II, alveolar macrophages, PMNs, endothelial cells
Emphysema	Protease–antiprotease imbalance (alpha1-antitrypsin deficiency), oxidative stress, chronic inflammation	Chronic inflammation indicated by increased numbers of activated macrophages, $CD8^{+}$, and PMNs; enlargement of distal air spaces, protease–antiprotease	*First-generation:* IT injection of elastases (papain)[134,135] See Antunes and Rocco Review[136] *Protease models:* IT injection of human neutrophilic elastase, papain induces panacinar emphysema.	None	Macrophages, PMNs, AEC I, natural ECM

(continued)

Table 3 Continued

Major categories of lung disease	Causes	Pathology to be modeled	Animal model	*In vitro* model	Cells needed for model
		imbalance, inactivation of antiproteases through oxidative stress, destruction of alveolar walls, pulmonary cachexia *Panacinar emphysema:* dilation and enlargement of the acini from the respiratory bronchioles to the alveoli; associated with alpha1-antitrypsin deficiency *Centrilobular emphysema*: inflammation and/or destruction of central or proximal acini comprised primarily by respiratory bronchi; distal acini formed by alveoli remain intact; associated with cigarette smoke exposure Irregular emphysema:	*Smoke exposure*: Exposure of animals to cigarette smoke induces centrilobular emphysema accompanied by an influx of inflammatory cells, weight loss, and systemic inflammation. *Disadvantage*: Species dependent oxidant-antioxidant responses (ascorbate metabolism and pulmonary glutathione)[137] could make animal studies unreliable for studying effects of oxidative stress on the pathogenesis of emphysema.		
Sarcoidosis	Unknown etiology	Noncaseating granulomas of tightly clustered epitheloid cells and giant cells encased by fibrous rims or hyaline scars, hilar lymphadenopathy, asteroid bodies within giant cells, Schaumann bodies, CD4:CD8 interstitial ratio of 5:1, increased IL-2, IFN-γ, IL-8, TNF, MIP-1α	*Mouse*: IT instillations of nanotubes in both WT and macrophage specific PPARgamma KO mice caused increased granuloma formation sixty days post-instillation in PPARgamma KO compared to WT mice[138]	None	$CD4^+$, $CD8^+$, macrophages
Bronchiolitis obliterans (BO)	Persistent obstructive bronchiolitis after an episode of acute bronchiolitis	Brochial and goblet cell metaplasia and/or dysplasia, narrowing of bronchioles due to mucus plugs, inflammation, fibrosis	*Rat*: 1) Wistar rats with IT injection of nitric acid formed lesions that constricted small airways. By day 2, bronchiolar lesions developed accompanied by alveolar hemorrhage, congestion, neutrophil accumulation, and alveolar edema. Histological specimens on day 7 showed bronchiolar epithelial metaplasia, foamy macrophages, and neutrophilic pneumonia. On day 14 alveolar bronchiolization and atelectasis were observed, and on day 30 atelectasis, mononuclear infiltrations and fibrosis were noted[139]	*Microfluidics*: Cellular injury of distal airways was modeled on a microchip with an air interface chamber lined with small airway epithelial cells (SAEC) and a vascular compartment lined with endothelial cells. Liquid plugs were injected into the SAEC chamber followed by introduction of a higher pressure air bubble to pop the liquid plug. Cell viability decreased with the number of liquid plugs run through the	Goblet cells, NHBE, PMNs, macrophages

(continued)

Table 3 Continued

Major categories of lung disease	Causes	Pathology to be modeled	Animal model	*In vitro* model	Cells needed for model
			2) IT diacetyl (DA) injection into male Sprague-Dawley rats induced severe necrosis and sloughing of the bronchiolar epithelial on day 1 accompanied by inflammatory cell infiltrates (PMNs, eosinophils, lymphocytes, histiocytes). Days 3 through 7 showed intraluminal fibrotic lesions and polypoid growth in bronchioles[140]	chamber. However, pure liquid surfactant flowed by an air bubble completely eliminated cellular injury seen with the nonsurfactant liquid plug[141]	
Bronchiectasis	Congenital/hereditary (cystic fibrosis, intralobar sequestration of the lung, primary ciliary dyskinesia), immunodeficiency with recurrent infections, postinfectious (*mycobacterium tuberculosis, Staphylococcus aureus, Haemophilus influenza, Pseudomonas*, adenovirus, influenza virus, HIV, *Aspergillus*), tumor, foreign body, chronic lung rejection, lupus, rheumatoid arthritis	Permanent bronchiole dilation due to destruction of elastin and smooth muscle around bronchi and bronchioles; mucosal biopsies contain neutrophils, T-lymphocytes, TNFα, elastase[142] desquamation of epithelial lining; necrosis; fibrosis most severe in lower lobes and vertical airways	*Mucus plug:* After 4 weeks rats exposed to sulfur dioxide vapor at doses of 300-400 ppm 5 h per day, 5 days showed goblet cell hyperplasia mucus hypersecretion in distal bronchioles and alveoli[143] *Cystic fibrosis*: 1, Transgenic pig[144,145] 2. Transgenic mouse[146,147] *Primary ciliary dyskinesia*[148] 1. *Dogs*: naturally occurring ciliary defects in springer spaniels and English setters 2. *Murine models*: X-linked recessive WIC-Hyd rat; *iv/iv, inv/inv,* and *hpy/hop* mice 3. *Pigs*: naturally occurring phenotypes of immotile cilia	None	PASMC, NHBE, cartilaginous 3D ECM
Chronic interstitial lung disease	Fibrosing, eosinophilic, drug reactions, radiation pneumonitis, granulomatous (sarcoidosis and hypersensitivity pneumonitis)	*Fibrosing*: cobblestoned lung due to retraction scars in intralobular septa, patchy interstitial fibrosis with fibroblastic foci, eventual collapse of alveolar walls, hyperplastic AEC II and bronchiolar epithelium, squamous	*Bleomycin*: IT instillation of bleomycin in murine models induces fibrosis[149–151] *Disadvantages*: Strain-related differences in mouse bleomycin hydrolase expression[152,153] could cause variable fibrosis reactions in mouse studies.	None	AEC II, AEC I, fibroblasts, macrophages

(continued)

Table 3 Continued

Major categories of lung disease	Causes	Pathology to be modeled	Animal model	*In vitro* model	Cells needed for model
		metaplasia, lymphocyte infiltrate, secondary PAH	*Left ventricular failure:* Ligation of the aorta in mice causes massive pulmonary remodeling including PF and PAH[154] *Diphtheria toxin*: Intrapulmonary injection of whole diphtheria toxin into genetically engineered mice with DTR-expressing AEC II selectively targets AEC II for cellular injury and induces fibrosis[155,156]		
Pneumoconiosis	Mineral dusts, silica, asbestos, beryllium, iron oxide	Recruitment of macrophages *Coal dust*: anthracosis, macules, fibrosis *Silicosis*: slow progressing, nodular, fibrosis, eggshell calcifications, lipoproteinaceous accumulations *Asbestos*: localized fibrous plaques, parenchymal interstitial fibrosis with asbestos bodies, enlarged honeycombed airspaces, pleural effusions, parietal pleural plaques, carcinogenic (mesotheliomas, carcinoma of lung, larynx, stomach, colon) Two geometric forms of asbestos: 1. Serpentine-curly and flexible; chrysotile chemical more soluble 2. Amphibole-straight, stiff, brittle; less prevalent but more carcinogenic, distal airways and can penetrate interstitium	*Silicosis models*: IT installation of particulate matter: 1. Rats BAL at 24 h, 1 week, 1 month, and 3 months showed an increase in immune cells. The highest PMN cell count was 24 h postinstillation[157] 2. Male Wistar rats sacrificed at 7, 15, or 30 days showed nodular fibrosis and fibroblast proliferation. Significantly higher ROS levels were seen at days 7 and 15[158] See Mossman[159] and Liu[160] for asbestos reviews *Asbestos*: Rats were exposed to asbestos for 1 h and sacrificed at 0, 5, 24 h, and 4 and 8 days. The highest concentrations of asbestos fibers were seen at terminal bronchioles[161] *Disadvantage*: Interaction with particles varies due to dimensions and architecture differences across species.[159]	*Silicosis 2D model*: Immortalized cell lines (BEAS-2B, A549, NHBE) induced cytokine response to silica matter in 2D culture[162] *Asbestos 2D model*: Cell-fiber interactions in A549 cultured with amphibole fibers was dependent on the morphology of amphibole fiber[163] Asbestos deposition density was greatest at airway bifurcations in a human lung cast exposed to aerosolized crocidolite asbestos[164]	Macrophages, AEC I, AEC II, fibroblasts
Pulmonary hypertension	*Primary*: BMPR2 signaling pathway defect (heterozygous mutation) *Secondary*: obstructive/interstitial diseases, heart disease, recurrent pulmonary emboli, autoimmune	Arterioles and small arteries (40–300 μm) affected; medial hypertrophy, intimal fibrosis *Indication of advanced stages*: plexogenic pulmonary arteriopathy (tuft of capillary formations spanning dilated artery lumens)	*BMPR2 transgenic mice:* BMPR2 transgenic mice exposed to hypoxic conditions developed mild intimal arterial thickening and PAH after 5 weeks[165] *Monocrotaline (MCT)*: IV injected MCT injures pulmonary endothelial cells and induces pulmonary smooth muscle hypertrophy in arteries of all sizes[166,167]	None	PASMC, endothelial, intimal fibroblasts

(continued)

Table 3 Continued

Major categories of lung disease	Causes	Pathology to be modeled	Animal model	*In vitro* model	Cells needed for model
	disorders (systemic sclerosis), toxin induced, high-altitude		*Hypoxia*: Rats exposed to 4 weeks of hypoxia showed slight pulmonary vascular remodeling, intimal and medial thickening and right ventricular hypertrophy[167] *Disadvantage*: Both models lack plexogenic lesion formation, minimal vascular smooth muscle proliferation, strain-dependent variability in mice[166] *Left ventricular failure:* Ligation of aorta in mice caused massive pulmonary remodeling leading to PF and PAH[168] *SU5416 plus hypoxia*: VEGFR inhibitor, SU5416, in the presence of hypoxia in rat model leads to PASMC proliferation and intimal and medial thickening of pulmonary arteries[169,170] *Disadvantage*: SU5416 model was not reproducible in mice[169]		
Respiratory tract infections	Influenza A virus infections (2009 H1N1)	Airway inflammation, edema, epithelial necrosis, hyaline membranes, diffuse alveolar damage, and hemorrhage	*2009 H1N1:* Ferrets (*Mustela putorius furo*) inoculated intranasally with influenza A/Netherlands/602/2009 (2009 A/H1N1 virus). Viral replication in both upper and lower respiratory tracts[171]	*2009 H1N1:* Ex vivo cultures of human conjunctiva, nasopharynx, bronchus, and lung, as well as in vitro cultures of human nasopharyngeal, bronchial, and alveolar epithelial cells. Cells exposed to A/HongKong/415742/09 (H1N1pdm) and various other strains of seasonal and avian influenza viruses[103]	Bronchial epithelial cells, alveolar epithelial cells
Pulmonary infections	Parainfluenza virus infections Respiratory syncytial virus (RSV) infections Influenza A virus infections (H5N1) Tuberculosis–*Mycobacterium tuberculosis* infections	Airway inflammation, necrosis and sloughing of respiratory epithelium, edema, excessive mucus production which obstructs flow in the small airways, and interstitial infiltration of the lung.	*Parainfluenza virus:* Transgenic mice (one with B6C3 background and the other with BALB/c background) that ubiquitously express human STAT2. Intranasal inoculation of mice with Parainfluenza virus 5 (PIV5) results in the blocking of IFN signaling[172] *RSV:* BALB/c mice infected with RSV A-2 strain. Mice developed acute pneumonia (peak days, 4–5) and chronic pulmonary inflammatory infiltrates that lasted up to 154 days[173]	*Parainfluenza virus:* human pseudostratified mucociliary airway epithelium (HAE) cultured on Transwell-Col inserts and exposed to human recombinant parainfluenza virus type 3 (rPIV3) that expresses GFP[104] *RSV:* Well-differentiated primary pediatric bronchial epithelial cells (WD-PBECs) cultured on collagen-coated	Bronchial epithelial cells, alveolar epithelial cells, pulmonary endothelial cells, PMNs

(continued)

Table 3 Continued

Major categories of lung disease	Causes	Pathology to be modeled	Animal model	*In vitro* model	Cells needed for model
			H5N1: Cynomolgus macaques (*Macaca fascicularis*) infected with influenza virus H5N1 (A/Hong Kong/156/97) developed acute respiratory distress syndrome and fever associated with a necrotizing interstitial pneumonia[174] Disadvantage: Size, cost and ethical considerations limit the use of this species in many settings *Mycobacterium tuberculosis:* BLT humanized mice with a NOD-SCID/ γc^{null} background. Mice were infected intranasally with M.tb strain (tdTomato H37Rv). Sites of infection in the lung were characterized by the formation of organized granulomatous lesions, caseous necrosis, bronchial obstruction, and human T cell distribution at sites of inflammation[175]	membranes in transwells at an air–liquid interface. WD-PBECs were infected with RSV strain A2 or a recent clinical isolate, BT2a[176] *H5N1 in vitro model:* Polarized primary human alveolar epithelial cells and lung microvascular endothelial cells grown in transwell culture inserts to compare infection via apical or basolateral surfaces. Cells infected with H5N1 virus (A/HongKong/483/97) and a representative seasonal influenza virus (A/Hong Kong/54/98)[105] *Mycobacterium tuberbulosis:* Cellular aggregates of human PBMCs infected with Mtb to model granuloma formation[89]	
Pneumonia	Viral: Influenza A viruses (H1N1, H7N9) Bacterial: *Streptococcus pneumonia* *Francisella tularensis*	Alveoli become inflamed and filled with fluid or pus; viral directed cell lysis, inflammatory infiltrates, capillary and small vessel thromboses Epithelial necrosis of the airways with submucosal chronic inflammation.	*Influenza A:* H1N1: Intratracheal inoculation of ferrets with H1N1 strains (A/Bilthoven/3075/1978 and A/Netherlands/26/2007) and H3N2 strains (A/Bilthoven/16190/1968 and A/Netherlands/177/2008) of seasonal influenza virus. Histologic examination revealed moderate to severe necrotizing bronchointerstitial pneumonia, severe edema, necrosis of alveolar epithelium, inflammatory infiltrates in alveolar septa and lumina[177] BALB/c mice inoculated intranasally with A/Anhui/1/2013 (H7N9) virus[178] Ferrets (Mustela putorius furo) are susceptible to both human and avian influenza viruses. Inoculated intranasally with A/Anhui/1/2013 (H7N9) virus[179] Disadvantage: Limited availability of ferret-specific reagents	*In vitro models of pneumonia:* Calu-3 cell monolayers were established on membranes in a two-chamber culture system. *Escherichia coli* incubated with either polyclonal SIgA or IgG was inoculated into the apical chamber and PMNs added to the basal chamber[106]	Alveolar epithelial cells, bronchial epithelial cells, endothelial cells PMNs

(continued)

Table 3 Continued

Major categories of lung disease	Causes	Pathology to be modeled	Animal model	*In vitro* model	Cells needed for model
			S. pneumonia models: CBA/J mouse model of penicillin-resistant pneumonia. Mice were intranasally challenged and were susceptible to several clinical isolates of *Streptococcus pneumoniae*, including four of five penicillin-susceptible and all five penicillin-resistant strains tested[178] Sprague-Dawley rat model of low-inoculum *Streptococcus pneumoniae* infection. Challenged via intraperitoneal or intrapulmonary injection with serotypes 1, 3, 4, 5, 6b, 7f, 9v, 14, 19f, and 23f[180] *F. tularensis models:* New Zealand White (NZW) rabbits exposed to aerosols containing *F. tularensis* strain SCHU S4. Pathophysiology of pneumonic tularemia in rabbits resembles what has been reported for humans[181]		
Other infection models	Hanta virus pulmonary syndrome (HPS): Andes virus SARS virus infections Middle eastern respiratory syndrome (MERS): MERS coronavirus (MERS CoV)	HPS → Diffuse bilateral interstitial pulmonary infiltrates Vascular leakage leading to interstitial pneumonitis, mononuclear cell infiltration, fibrin deposition and focal hyaline membranes SARS infection(Diffuse alveolar damage with multinucleate giant- cells and a prominent increase of macrophages in the alveoli and lung interstitium MERS infection(Severe pneumonia, multiorgan dysfunction	Hanta virus pulmonmary syndrome: Syrian hamsters challenged with ANDV, strain Chile-9717869 and various other Andes virus strains. Rapidly progressing respiratory distress and pathologic findings closely resemble HPS in humans[182] *SARS virus:* BALB/c mice were exposed to SARS-CoV (Urbani isolate) intranasally. Mice showed elevated levels of pro-inflammatory cytokines, alveolar damage, and interstitial pneumonitis[183] *MERS CoV:* Rhesus macaques were exposed to MERS-CoV isolate HCoVEMC/2012 by intratracheal, ocular, oral, and intranasal inoculation. They developed a transient lower respiratory infection[184]	*HPS:* None *SARS:* A549 and THP-1 cells in an *in vitro* assay system to compare the responses of both lung epithelial cells and monocytic cells to SARS-CoV and to CoV-229E[185] *MERS-CoV:* Human monocyte-derived macrophages and *ex vivo* lung tissues were exposed to a clinical isolate of MERS-CoV. The virus can establish a productive infection in human macrophages and lead to an aberrant induction of inflammatory cytokines[186]	Bronchial epithelial cells alveolar epithelial cells, endothelial cells, lymphocytes
Lung transplantation	Acute rejection	Acute rejection: T lymphocyte recognition of foreign human leukocyte antigens (HLA); lymphocyte inflammatory response centered on blood vessels and/or airways	Acute rejection: Lung transplantation performed between BALB/c (donor) and C57BL/6 (recipient) mice. At day 5 after transplantation, lung allografts were recovered for SEM and for histologic analysis[187]	None	Lymphocytes, lung tissue from different donors/sources that is not HLA matched

reliance on animal models fails to give an accurate picture of immune cascades and fails to allow for easy identification of key factors leading to endothelial injury or vascular permeability. Interestingly, animal models using IL-2 injection were based on the observation that IL-2 was linked to vascular leak syndrome and subsequent development of pulmonary edema. Previous studies indicated that IL-2 itself does not activate vascular leakage, but rather IL-2 induces a cytokine cascade resulting in elevated levels of interferon-gamma, tumor necrosis factor (TNF), lymphotoxin, and IL-1 leading to endothelial activation and subsequent leakage.[188–191] A complex immune signaling cascade was thought to be necessary in order to induce vascular permeability making animal models appealing tools for studying development of pulmonary edema. The exact role of IL-2 in vascular permeability is now being elucidated using an *in vitro* microfluidics model of pulmonary edema developed by Huh *et al*.[5] They determined that IL-2 alone was enough to cause vascular leakage. Their lung-on-a-chip microfluidics model separates alveolar and vascular compartments by separating parallel microchannels on the microchip with a porous membrane. Mimicking the alveolar–vascular interface, a single layer of human endothelial cells was cultured in one microchannel filled with fluid, and human type I AECs were cultured in the other air filled microchannel. To induce vascular injury IL-2 was administered through the plasma filled vascular compartment lined with endothelial cells. Fibrin clots were seen in the alveolar microchannel after the administration of IL-2 in the vascular compartment indicating that IL-2 induced vascular and type I AEC permeability through the leakage of fibrin from the vascular microchannel over to the alveolar microchannel. Co-administration of IL-2 with an agent known to prevent vascular leakage, Ang-1, prevented vascular leakage and pulmonary edema illustrating that the microchip offers an elegant solution for high-throughput drug screening in addition to eliminating complex variables seen in *in vivo* studies.[5] Another animal model of pulmonary edema via microvascular injury used a similar strategy of toxin-induced injury and injected lipopolysaccharide (LPS) intravenously into the tail vein of Wistar rats to observe the effects on the endothelium of the lung. Vascular permeability increased and neutrophil activity peaked 30–60 min postinjection.[132] The scope of this model extends beyond the study of pulmonary edema. Injecting LPS has also been used for sepsis models in animals as well as for modeling DAD. In relation to pulmonary edema, however, it is unclear as with IL-2 what the key factors are for inducing vascular leakage with LPS. LPS is known to trigger an innate immune response via Toll like receptor-4 (TLR-4) on macrophages, but it is possible that either direct interaction of immune cells with the endothelium or indirect cytokine signaling induces vascular leakage. Additionally, TLR-4 in rats and mice recognize different LPS molecules than human TLR-4.

Current models of BO

Animal models of BO attempt to induce cellular injury through instillations of a toxic substance into the trachea of rats, using either diacetyl or nitric acid.[139,140] In these models, bronchial epithelial cell metaplasia and dysplasia were seen along with some inflammatory immune response. After 14 days of intratracheal exposure to nitric acid, atelectasis was observed in Wistar rats, and after 7 days of intratracheal exposure to diacetyl, intraluminal-induced fibrotic lesions were seen in Sprague-Dawley rats. However, these animal models generated variable results. Nitric acid exposure elicited alveolar hemorrhages while diacetyl exposed rats demonstrated no hemorrhaging but induced eosinophilic infiltrate which was not detected in nitric acid exposure. Developing an *in vitro* model for BO may lead to a better understanding of pathogenesis and may help to reduce variability of model responses.

So far, a current microfluidics approach to disease modeling has provided insight into how an *in vitro* model could be used to study cellular injury in diseases such as BO. An *in vitro* model has been developed to test cellular injury after the introduction of mucus plugs in small airways. Tavana *et al.* used a microfluidics construct that contained an air chamber lined with small airway epithelial cells and a vascular compartment lined with endothelial cells.[141] Nonsurfactant liquid plugs were injected into the air chamber followed by the introduction of a higher pressure air bubble. Air pressure was continuously applied until the air bubble was popped. Interestingly, cellular viability decreased with the amount of nonsurfactant liquid plugs run through the chamber. However, surfactant liquid plugs had no effect on cell survival.[141] Although this model does not claim to be a model specifically for BO, the principles of cellular injury can be applied to epithelial injury seen in BO in the presence of mucus or liquid plugs.

Pneumoconiosis models

Numerous animal studies inject particulate matter into the trachea in order to determine the distribution and effects of mineral dusts, silica, and asbestos. Critically, examining the distribution patterns in animals may be misleading due to anatomical differences.[192–194] Rats, unlike humans, have a higher distribution of particulate in the alveolar region[195] whereas reconstructed 3D human airway lung casts demonstrate particle deposition is greatest at airway bifurcations.[196] Several 2D *in vitro* models using human cell lines have been used to study cellular response to particulate exposure. Not surprisingly, incubating cultured cells with silica matter induced a cytokine response,[195] and cell–amphibole asbestos fiber interaction was dependent on the morphology of the amphibole fiber.[197] One dynamic *in vitro* model of particulate exposure incubated A549 cells on stretchable scaffolds. Cellular scaffolds were composed either of fibronectin or collagen I and cells were seeded over the constructs. When glass or asbestos particles were incubated with A549 cells, a significant increase in interleukin-8 (IL-8) secretion was seen in the dynamically stretched cultures compared to static cultures. Critically, the dynamic stretching appeared to cause repeated mechanical cellular damage.[198]

Other lung disease models

Currently, no *in vitro* human models exist for the study of DAD, emphysema, sarcoidosis, bronchiectasis, chronic interstitial lung disease, or pulmonary hypertension although the pathology of each of these diseases and current animal model data provide the critical information necessary for the generation of these respiratory tissue models (Table 3).

Existing infectious disease models

A number of *in vitro* physiologic models of human airway epithelium and lung have been produced but few have been used to examine human responses following exposure to microbial pathogens (Table 3). Human lung tissue models, or models of other tissues, are also exceptionally suitable for use in the study of microbial pathogenesis of biohazardous agents which require work to be done in high and maximum biocontainment where the use of animals is problematic. Animal models often do not adequately replicate responses or pathogenesis seen in human disease.[199] Human 3D tissue models have great potential for use in the examination of lung disease pathogenesis and host response to biohazardous agents such as the recently emerged avian influenza A H7N9 virus, severe acute respiratory syndrome (SARS)-like respiratory virus,[200] and Middle Eastern Respiratory Syndrome Corona virus (MERS-CoV).[186] In the future human 3D lung tissue models will provide a means for systematic, repetitive, and quantitative evaluations of human lung disease and a modality to examine drug responses. *Ex vivo* cultures of nasopharynx, bronchus, and lung, as well as in vitro cultures of human nasopharyngeal, bronchial, and AECs have been exposed to A/HongKong/415742/09 (H1N1pdm) and various other strains of seasonal and avian influenza viruses[103] but development of respiratory infectious disease models has been limited. One pathologic model used cellular aggregates of human peripheral blood mononuclear cells exposed to *Mycobacterium tuberculosis* to examine cellular and immunological responses during granuloma formation in the lung.[89] Models have also been developed to examine human cell exposure to parainfluenza virus type 3,[104] respiratory syncytial virus,[176] and H5N1 avian influenza A.[105] *In vitro* models of pneumonia,[106] SARS virus,[200] and MERS-CoV[186] have been shown to re-create components of human disease pathogenesis following exposure to these microbial pathogens.

Cancer models

Models that recapitulate aspects of the genesis, progression, and clinical course of human cancers are valuable resources to cancer researchers to support a variety of basic, translational, and clinical investigations. Efforts have just begun to use tissue mimics to identify biomarkers of disease progression and outcome, to understand mechanisms of drug action, to investigate the usefulness of novel drug combinations, and to study mechanisms of cancer metastases and drug resistance. Table 4 lists some of the current animal models as well as *in vitro* models for cancer. A few 2D models have been produced but these lack the cellular adhesions, morphology, or migration patterns seen in human cancers *in vivo*.[1,2] Studies have also shown that 2D culture systems also do not react the same way that 3D systems do. A549 cells grown on 3D ECM, composed of laminin and fibronectin, displayed enhanced radioresistance as compared to 2D cultured cells when exposed to ionizing radiation.[201] Bronchial epithelial fragments from patient biopsies were cut (to expose basement membrane) and then placed in agar culture wells coated with the tumor cell line EPLC32M1. In this model tumor cell attachment was seen in all exposed basement membranes biopsies.[202] In another *in vitro* cancer model AC 6 wk/o natural lung rat scaffolds were seeded with 25 million A549 cells and cultured in order to evaluate nodule formation. Microarray analysis showed gene expression differences of A549 cells cultured in 2D versus 3D (matrigel) versus 4D (AC scaffold).[53]

It has been difficult to replicate the cancer microenvironment in a model. The ability to use a model to rapidly generate many tumor cells from small biopsy specimens or from frozen tissue would provide significant opportunities for development of patient-specific cell-based diagnostics in the future. Just like other lung model systems, a microfluidic lung cancer model must address the complexity of the natural environment in order for it to be clinically relevant. Models should also support growth of tumors, tumor angiogenesis, and maintain the cells in their natural proliferative state. HoC cancer models might even be able to examine metastasis and invasion of tumors into surrounding normal tissue. Current microfluidic and systems for support of lung cancer models do not exist and must be developed in the future. Advances in generation of fluidic systems to maintain HoC may eventually lead to production of systems that could be applied to support of lung cancer models as well.

Concluding remarks

During the last 10 years a great deal of progress has been made in developing technologies that identify events occurring in early stages of lung disease. Among those developing technologies has been the realization that 2D μlung and 3D HoC culture systems can be produced which better mimic the physiologic parameters within normal tissues compared to traditional plate culture systems or even animal models. By approximating human disease states and pathologic mechanisms of drug-induced lung disorders these models will allow us to identify adverse drug reactions, potential pulmonary complications such as drug-induced angioedema, or even responsiveness of drugs well before initiation of clinical trials.

In this paper we have summarized the early development of respiratory tract models. We have also discussed the pros and cons for the use of specific cell types that populate these systems and their contribution to the development of lung models. Recently, technological advancements have resulted in the generation of lung-on-a-chip devices with microfluidic support systems that can mimic specific disease states such as pulmonary edema or other structural components that are responsible for a

Table 4 Current cancer models

	Cell lines currently used in lung cancer models	Cancer microenvironment	Pulmonary cancer types (short list)	Animal models	Human *in vitro* models	Cells to use in future models
Cancer	Adenocarcinoma human alveolar basal epithelial cells: A549, NCI H125 Malignant squamous cell carcinoma: EPLC32M1 Malignant large cell carcinoma found in pleural effusion: LCLC103H	See Hanahan Hallmarks of Cancer[203] Microenvironment (stiffness and ligands of ECM, chemokines, growth factors, cell–cell interactions): • enhances survival mechanisms; • induces EMT (migration); • Induces proliferation; • alters signaling pathways • gene expression differences • macrophages and fibroblasts enhance metastasis and migration Two types of ECM: basement membrane and interstitium.	*Squamous cell carcinoma:* bronchial mucosa. Correlated with smoking hx, keratinization of epithelia. Highest frequency of p53 mutation *Adenocarcinoma*: malignant epithelial tumor with glandular differentiation, more common in women and nonsmokers, K-RAS mutations *Bronchioloalveolar carcinoma*: pulmonary parenchyma, nodules, pneumonia like consolidation.	See Kwon (2013) Table 1 for review[204] *Genetic mouse models*: 1. Kras mutation: adenocarcinomas 2. EGFR mutation: bronchioalveolar carcinoma 3. Adenoviruses (Ad5 SPC-Cre and Ad5-CC10-Cre): adenocarcinoma in both CC10-positive and SPC-positive cells 3. Inactivation of Rb or p53 with lentiviral or adenoviral vectors expressing Cre recombinase leads to SCLC in mice. *Xenograft models*:1. A549 cells inoculated subcutaneously into right flank of BALB/c-nu male mice[205] 2. Harvested primary human lung adenocarcinoma (201T) cells and injected into the lumen of bronchial xenografts placed on the flank of SCID mice. Minimal invasiveness into submucosa[206] 3. Pt derived ex vivo non-small cell lung cancer inoculated subcutaneously on SCID mice[207]	*2D*: Does not mimic *in vivo* cellular adhesions, morphology, or migration[1,2] *3D*: 1. A549 cells grown on 3D ECM, composed of laminin and fibronectin, displayed enhanced radioresistance when exposed to ionizing radiation[208] 2. Bronchial epithelial fragments from patient biopsies were placed or cut (to expose basement membrane) then placed in agar culture wells coated with tumor cell line EPLC32M1. Tumor cell attachment was seen in all exposed basement membranes biopsies[202] 3. AC 6 weeks/o rat scaffold, seeded with 25 million A549 cells → Nodule formation. Microarray showed gene expression differences of A549 cells cultured in 2D versus 3D (matrigel) versus 4D (AC scaffold)[53]	Patient derived primary tumor cells from different cancer types, fibroblasts, cancer associated macrophages

pathologic response. This is a major development in the field and although these technologies are relatively new, are not commercially available, and have not been standardized or validated, they have great potential to aid in predicting human respiratory tract responses and pathologic mechanisms of disease. By approximating human disease states and pathologic mechanisms of drug-induced lung disorders these models will allow us to identify adverse drug reactions, potential pulmonary complications such as drug-induced angioedema, or even responsiveness of drugs well before initiation of clinical trials. In the future we hope to use human respiratory tissue models in all stages of drug development from disease modeling to prediction of drug targets and finally in preclinical toxicity testing. This should accelerate the early steps in drug discovery, reduce the cost of drug development, bring drugs to clinical trials at earlier stages, and at the same time enhance our ability to select drugs appropriate for human use.

Author contributions: All authors participated in the design and production of this manuscript as a whole. JEN, JC, and JAN supplied the format and final review of the entire manuscript. JEN and LBA designed and produced Table 1 regarding options for cell types. JEN and SPV designed and produced Table 2 reviewing all current lung models. JEN, AE, and JC designed and produced Table 3 reviewing current human lung diseases, pathology, animal models and *in vitro* lung models.

ACKNOWLEDGEMENTS

We would like to thank John D. Barajas for his graphic arts skills related to preparation of Figure 1 in this manuscript. We would like to thank Dr. Scott Moen for producing the microfluidic lung slide system presented in Figure 1 of this manuscript. The research described and the preparation of this manuscript was funded in part through the NIH Common Fund, NCATS U18 grant, Grant No. 1-U18-TR-000560.

REFERENCES

1. Hakkinen KM, Harunaga JS, Doyle AD, Yamada KM. Direct comparisons of the morphology, migration, cell adhesions, and actin cytoskeleton of fibroblasts in four different three-dimensional extracellular matrices. *Tissue Eng Part A* 2011;**17**:713–24
2. Eke I, Cordes N. Radiobiology goes 3D: how ECM and cell morphology impact on cell survival after irradiation. *Radiother Oncol* 2011;**99**:271–8
3. Cortiella J, Niles J, Cantu A, Brettler A, Pham A, Vargas G, Winston S, Wang J, Walls S, Nichols JE. Influence of acellular natural lung matrix on murine embryonic stem cell differentiation and tissue formation. *Tissue Eng Part A* 2010;**16**:2565–80
4. Wikswo JP, Curtis EL, Eagleton ZE, Evans BC, Kole A, Hofmeister LH, Matloff WJ. Scaling and systems biology for integrating multiple organs on a chip. *Lab Chip* 2013;**13**:3496–511
5. Huh D, Leslie DC, Matthews BD, Fraser JP, Jurek S, Hamilton GA, Thorneloe KS, McAlexander MA, Ingber DE. A human disease model of drug toxicity-induced pulmonary edema in a lung-on-a-chip microdevice. *Sci Transl Med* 2012;**4**:1–8
6. Lechner JF, Haugen A, Autrup H, McClendon IA, Trump BF, Harris CC. Clonal growth of epithelial cells from normal adult human bronchus. *Cancer Res* 1981;**41**:2294–304
7. Hoang ATN, Chen P, Juarez J, Sachamitr P, Billing B, Bosnjak L, Dahlén B, Coles M, Svensson M. Dendritic cell functional properties in a three-dimensional tissue model of human lung mucosa. *Am J Physiol Lung C* 2012;**302**:L226–37
8. Ramirez RD, Sheridan S, Girard L, Sato M, Kim Y, Pollack J, Peyton M, Zou Y, Kurie JM, Dimaio JM, Milchgrub S, Smith AL, Souza RF, Gilbey L, Zhang X, Gandia K, Vaughan MB, Wright WE, Gazdar AF, Shay JW, Minna JD. Immortalization of human bronchial epithelial cells in the absence of viral oncoproteins. *Cancer Res* 2004;**64**:9027–34
9. Twort C, Van Breemen C. Human airway smooth muscle in culture. *Tissue Cell* 1988;**20**:339–44
10. Choe MM, Sporn PH, Swartz MA. Extracellular matrix remodeling by dynamic strain in a three-dimensional tissue-engineered human airway wall model. *Am J Res Cell Mol* 2006;**35**:306
11. Ebina M, Takahashi T, Chiba T, Motomiya M. Cellular hypertrophy and hyperplasia of airway smooth muscles underlying bronchial asthma: a 3-D morphometric study. *Am Rev Respir Dis* 1993;**148**:720–6
12. Knox AJ, Corbett L, Stocks J, Holland E, Zhu YM, Pang L. Human airway smooth muscle cells secrete vascular endothelial growth factor: up-regulation by bradykinin via a protein kinase C and prostanoid-dependent mechanism. *FASEB J* 2001;**15**:2480–88
13. Cozens AL, Yezzi MJ, Kunzelmann K, Ohrui T, Chin L, Eng K, Finkbeiner WE, Widdicombe JH, Gruenert DC. CFTR expression and chloride secretion in polarized immortal human bronchial epithelial cells. *Am J Res Cell Mol* 1994;**10**:38–47
14. Masui T, Wakefield LM, Lechner JF, LaVeck MA, Sporn MB, Harris CC. Type beta transforming growth factor is the primary differentiation-inducing serum factor for normal human bronchial epithelial cells. *Proc Natl Acad Sci* 1986;**83**:2438–42
15. Forbes B, Shah A, Martin GP, Lansley AB. The human bronchial epithelial cell line 16HBE14o − as a model system of the airways for studying drug transport. *Int J Pharm* 2003;**257**:161–17
16. Ehrhardt C, Kneuer C, Laue M, Schaefer UF, Kim KJ, Lehr CM. 16HBE14o-human bronchial epithelial cell layers express P-glycoprotein, lung resistance-related protein, and caveolin-1. *Pharm Res* 2003;**20**:545–51
17. Fogh J, Fogh JM, Orfeo T. One hundred and twenty-seven cultured human tumor cell lines producing tumors in nude mice. *J Natl Cancer* 1977;**59**:221–6
18. Cavet ME, West M, Simmons NL. Transepithelial transport of the fluoroquinolone ciprofloxacin by human airway epithelial Calu-3 cells. *Antimicrob Agents Chemother* 1997;**41**:2693–8
19. Florea BI, Cassara ML, Junginger HE, Borchard G. Drug transport and metabolism characteristics of the human airway epithelial cell line Calu-3. *J Control Release* 2003;**87**:131–8
20. Foster KA, Avery ML, Yazdanian M, Audus KL. Characterization of the Calu-3 cell line as a tool to screen pulmonary drug delivery. *Int J Pharm* 2000;**208**:1–11
21. Shen BQ, Finkbeiner WE, Wine JJ, Mrsny RJ, Widdicombe JH. Calu-3: a human airway epithelial cell line that shows cAMP-dependent Cl- secretion. *Am J Physiol Lung C* 1994;**266**:L493–50
22. Bell ET. Hyperplaisa of the pulmonary alveolar epithelium in disease. *Am J Pathol* 1943;**19**:901–11
23. Fulcher ML, Gabriel S, Burns KA, Yankaskas JR, Randell SH. Well-differentiated human airway epithelial cell cultures. In: Mitry RR and Hughes RD (eds) *Human cell culture protocols*. Humana Press, 2005, pp.183–206
24. Hackett TL, Warner SM, Stefanowicz D, Shaheen F, Pechkovsky DV, Murray LA, Argentieri R, Kicic A, Stick SM, Bai TR, Knight DA. Induction of epithelial–mesenchymal transition in primary airway epithelial cells from patients with asthma by transforming growth factor-β1. *Am J Res Crit Care* 2009;**180**:122–33
25. Giard DJ, Aaronson SA, Todaro GJ, Arnstein P, Kersey JH, Dosik H, Parks WP. In vitro cultivation of human tumors: establishment of cell lines derived from a series of solid tumors. *J Natl Cancer* 1973;**51**:1417–23
26. Foster KA, Oster CG, Mayer MM, Avery ML, Audus KL. Characterization of the A549 cell line as a type II pulmonary epithelial cell model for drug metabolism. *Exp Cell Res* 1998;**243**:359–66

27. Shapiro DL, Nardone LL, Rooney SA, Motoyama EK, Munoz JL. Phospholipid biosynthesis and secretion by a cell line (A549) which resembles type II alveolar epithelial cells. *BBA-Lipid Lipid Met* 1978;**530**:197–207
28. Jaffe EA, Nachman RL, Becker CG, Minick CR. Culture of human endothelial cells derived from umbilical veins. Identification by morphologic and immunologic criteria. *J Clin Invest* 1973;**52**:2745
29. Lidington EA, Moyes DL, McCormack AM, Rose ML. A comparison of primary endothelial cells and endothelial cell lines for studies of immune interactions. *Transpl Immunol* 1999;**7**:239–46
30. Unger RE, Krump-Konvalinkova V, Peters K, Kirkpatrick CJ. In vitro expression of the endothelial phenotype: comparative study of primary isolated cells and cell lines, including the novel cell line HPMEC-ST1. 6R. *Microvasc Res* 2002;**64**:384–97
31. Muanza K, Gay F, Behr C, Scherf A. Primary culture of human lung microvessel endothelial cells: a useful in vitro model for studying Plasmodium falciparum-infected erythrocyte cytoadherence. *Res Immunol* 1996;**147**:149–63
32. Hewett PW, Murray JC. Human microvessel endothelial cells: isolation, culture and characterization. *In Vitro Cell Dev Biol-Anim* 1993;**29**:823–30
33. Comhair SA, Xu W, Mavrakis L, Aldred MA, Asosingh K, Erzurum SC. Human primary lung endothelial cells in culture. *Am J Res Cell Mol* 2012;**46**:723
34. Hermanns MI, Fuchs S, Bock M, Wenzel K, Mayer E, Kehe K, Bittinger F, Kirkpatrick CJ. Primary human coculture model of alveolo-capillary unit to study mechanisms of injury to peripheral lung. *Cell Tissue Res* 2009;**336**:91–105
35. Jacobs JP, Jones CM, Baille JP. Characteristics of a human diploid cell designated MRC-5. *Nature* 1970;**227**:168–70
36. Boeckh M, Gleaves CA, Bindra R, Meyers JD. Comparison of MRC-5 and U-373MG astrocytoma cells for detection of cytomegalovirus in shell vial centrifugation cultures. *Eur J of Clin Microbiol* 1991;**10**:569–72
37. Hayflick L. The limited in vitro lifetime of human diploid cell strains. *Exp Cell Res* 1965;**37**:614–36
38. Kalimi M, Seifter S. Glucocorticoid receptors in WI-38 fibroblasts Characterization and changes with population doubling in culture. *BBA-Gen Subj* 1979;**583**:352–59
39. Allen RG, Tresini M, Keogh BP, Doggett DL, Cristofalo VJ. Differences in electron transport potential, antioxidant defenses, and oxidant generation in young and senescent fetal lung fibroblasts (WI-38). *J Cell Physiol* 1999;**180**:114–22
40. He Z, Huang S, Li Y, Zhang Q. Human embryonic stem cell lines preliminarily established in China. *Zhonghua Yi Xue Za Zhi* 2002;**82**:1314
41. Takahashi K, Tanabe K, Ohnuki M, Narita M, Ichisaka T, Tomoda K, Yamanaka S. Induction of pluripotent stem cells from adult human fibroblasts by defined factors. *Cell* 2007;**131**:861–72
42. Cox JL, Rizzino A. Induced pluripotent stem cells: what lies beyond the paradigm shift. *Exp Biol Med* 2010;**235**:148–58
43. Gunaseeli I, Doss MX, Antzelevitch C, Hescheler J, Sachinidis A. Induced pluripotent stem cells as a model for accelerated patient- and disease-specific drug discovery. *Curr Med Chem* 2010;**17**:759–66
44. O'Malley J. New strategies to generate induced pluripotent stem cells. *Curr Opin Biotech* 2009;**20**:516–21
45. Nichols JE, Niles J, Riddle M, Vargas G, Schilagard T, Ma L, Edward K, La Francesca S, Sakamoto J, Vega S, Ogedegbe M, Mlcak R, Devo D, Woodson L, McQuitty C, Lick S, Beckles D, Melo E, Cortilla J. Production and assessment of decellularized pig and human lung scaffolds. *Tissue Eng Part A* 2013;**19**:2045–62
46. Pugin J, Dunn I, Jolliet P, Tassaux D, Magnenat JL, Nicod LP, Chevrolet JC. Activation of human macrophages by mechanical ventilation in vitro. *Am J Physiol* 1998;**275**:L1040–50
47. Hermanns MI, Unger RE, Kehe K, Peters K, Kirkpatrick CJ. Lung epithelial cell lines in coculture with human pulmonary microvascular endothelial cells: development of an alveolar-capillary barrier in vitro. *Lab Invest* 2004;**84**:736–52
48. Huh D, Matthews BD, Mammoto A, Montoya-Zavala M, Hsin HY, Ingber DE. Reconstituting organ-level lung functions on a chip. *Science* 2010;**328**:1662–8
49. Ott HC, Clippinger B, Conrad C, Schuetz C, Pomerantseva I, Ikonomou L, Kotton D, Vacanti JP. Regeneration and orthotopic transplantation of a bioartificial lung. *Nat Med* 2010;**16**:927–333
50. Kloxin AM, Lewis KJ, DeForest CA, Seedorf G, Tibbitt MW, Balasubramaniam V, Anseth KS. Responsive culture platform to examine the influence of microenvironmental geometry on cell function in 3D. *Integr Biol (Camb)* 2012;**4**:1540–9
51. Patel H, Kwon S. Multi-walled carbon nanotube-induced inflammatory response and oxidative stress in a dynamic cell growth environment. *J Biol Eng* 2012;**6**:22
52. Horie M, Saito A, Mikami Y, Ohshima M, Morishita Y, Nakajima J, Kohyama T, Nagase T. Characterization of human lung cancer-associated fibroblasts in three-dimensional in vitro co-culture model. *Biochem Biophys Res Commun* 2012;**423**:158–63
53. Mishra DK, Creighton CJ, Zhang Y, Gibbons DL, Kurie JM, Kim MP. Gene expression profile of A549 cells from tissue of 4D model predicts poor prognosis in lung cancer patients. *Int J Cancer* 2013. Epub ahead of print 2013. DOI: 10.1002/ijc.28428
54. Blau H, Guzowski DE, Siddiqi ZA, Scarpelli EM, Bienkowski RS. Fetal type 2 pneumocytes form alveolar-like structures and maintain long-term differentiation on extracellular matrix. *J Cell Physiol* 1998;**136**:203–14
55. Chinoy MR, Antonio-Santiago MT, Scarpelli EM. Maturation of undifferentiated lung epithelial cells into type II cells in vitro: a temporal process that parallels cell differentiation in vivo. *Anat Rec* 1994;**240**:545–54
56. Chen P, Marsilio E, Goldstein RH, Yannas IV, Spector M. Formation of lung alveolar-like structures in collagen-glycosaminoglycan scaffolds in vitro. *Tissue Eng* 2005;**11**:1436–48
57. Mondrinos MJ, Koutzaki S, Jiwanmall E, Li M, Dechadarevian JP, Lelkes PI, Fink CM. Engineering three-dimensional pulmonary tissue constructs. *Tissue Eng* 2006;**12**:717–28
58. Mondrinos MJ, Koutzaki S, Lelkes PI, Finck CM. A tissue-engineered model of fetal distal lung tissue. *Am J Physiol Lung Cell Mol Physiol* 2007;**293**:L639–50
59. Andrade CF, Wong AP, Waddell TK, Keshavjee S, Liu M. Cell-based tissue engineering for lung regeneration. *Am J Physiol* 2007;**292**:L510–8
60. Price AP, England KA, Matson AM, Blazar BR, Panoskaltsis-Mortari A. Development of a decellularized lung bioreactor system for bioengineering the lung: the matrix reloaded. *Tissue Eng Part A* 2010;**16**:2581–91
61. Coraux C, Nawrocki-Raby B, Hinnrasky J, Kileztky C, Gaillard D, Dani C, Puchelle E. Embryonic stem cells generate airway epithelial tissue. *Am J Respir Cell Mol Biol* 2005;**32**:87–92
62. Cortiella J, Nichols JE, Kojima K, Bonassar LJ, Dargon P, Roy AK, Vacant MP, Niles JA, Vacanti CA. Tissue-engineered lung: an in vivo and in vitro comparison of polyglycolic acid and pluronic F-127 hydrogel/somatic lung progenitor cell constructs to support tissue growth. *Tissue Eng* 2006;**12**:1213–25
63. Zani BG, Kojima K, Vacanti CA, Edelman ER. Tissue-engineered endothelial and epithelial implants differentially and synergistically regulate airway repair. *Proc Natl Acad Sci U S A* 2008;**105**:7046–51
64. Nichols JE, LeDuc J. Influenza. In: Barrett ADT, Stanberry LR (eds) *Vaccines*. London, UK: Academic Press, 2009, pp. 498–515
65. Lin YM, Zhang A, Rippon HJ, Bismarck A, Bishop AE. Tissue engineering of lung: the effect of extracellular matrix on the differentiation of embryonic stem cells to pneumocytes. *Tissue Eng Part A* 2010;**16**:1515–26
66. Huang SX, Islam MN, O'Neill J, Hu Z, Yang YG, Chen YW, Mumau M, Green MD, Vunjak-Novakovic G, Bhattacharya J, Snoeck HW. Efficient generation of lung and airway epithelial cells from human pluripotent stem cells. *Nat Biotechnol* 2014;**32**:84–91
67. Ghaedi M, Calle EA, Mendez JJ, Gard AL, Balestrini J, Booth A, Bove PF, Gui L, White ES, Niklason LE. Human iPS cell-derived alveolar epithelium repopulates lung extracellular matrix. *J Clin Invest* 2013;**123**:4950–62
68. Mou H, Zhao R, Sherwood R, Ahfeldt T, Lapey A, Wain J, Sicilian L, Izvolsky K, Musunuru K, Cowan C, Rajagopal J. Generation of multipotent lung and airway progenitors from mouse ESCs and patient-specific cystic fibrosis iPSCs. *Cell Stem Cell* 2012;**10**:385–97

69. Nichols JE, Cortiella J. Engineering of a complex organ: progress toward development of a tissue-engineered lung. *Proc Am Thorac Soc* 2008;**5**:723–30
70. Nichols JE, Niles JA, Cortiella J. Design and development of tissue engineered lung. *Organogenesis* 2009;**5**:57–61
71. Nichols JE, Niles JA, Cortiella J. Production and utilization of acellular lung scaffolds in tissue engineering. *J Cell Biochem* 2012;**113**:2185–92
72. Choe MM, Tomei AA, Swartz MA. Physiological 3D tissue model of the airway wall and mucosa. *Nat Protoc* 2006;**1**:357–62
73. Miller C, George S, Niklason L. Developing a tissue-engineered model of the human bronchiole. *J Tissue Eng Regen Med* 2010;**4**:619–27
74. Singh D, Zo SM, Kumar A, Han SS. Engineering three-dimensional macroporous hydroxyethyl methacrylate-alginate-gelatin cryogel for growth and proliferation of lung epithelial cells. *J Biomater Sci Polym Ed* 2013;**24**:1343–59
75. Petersen TH, Calle EA, Zhao L, Lee EJ, Gui L, Raredon MB, Gavrilov K, Yi T, Zhuang ZW, Breuer C, Herzog E, Niklason LE. Tissue-engineered lungs for in vivo implantation. *Science* 2010;**329**:538–41
76. Crapo PM, Gilbert TW, Badylak SF. An overview of tissue and whole organ decellularization processes. *Biomaterials* 2011;**32**:3233–43
77. Lwebuga-Mukasa JS, Ingbar DH, Madri JA. Repopulation of a human alveolar matrix by adult rat type II pneumocytes in vitro: a novel system for type II pneumocyte culture. *Exp Cell Res* 1986;**162**:423–35
78. Liu Y, Singh AK. Microfluidic platforms for single-cell protein analysis. *J Lab Autom* 2013. Epub ahead of print 2013. DOI: 10.1177/2211068213494389
79. Delamarche E, Tonna N, Lovchik RD, Bianco F, Matteoli M. Pharmacology on microfluidics: multimodal analysis for studying cell-cell interaction. *Curr Opin Pharmacol* 2013;**13**:821–8
80. Ruiz SA, Chen CS. Microcontact printing: a tool to pattern. *Soft Matter* 2007;**3**:168–77
81. Sin ML, Gao J, Liao JC, Wong PK. System integration – a major step toward lab on a chip. *J Biol Eng* 2011;**5**:6
82. Ren K, Chen Y, Wu H. New materials for microfluidics in biology. *Anal Biotech* 2014;**25**:78–85
83. Arshad A. Drug-induced pulmonary toxicity workup. Medscape WebMD LLC 20 Nov 2013. http://emedicine.medscape.com/article/1343451-workup
84. Bonniaud Ph, Baudouin N, Fanton A, Camus C, Favrolt N, Guerriaud M, Jacquet L. The drug-induced respiratory disease website. Pneumotox On Line, http://www.pneumotox.com/
85. Sugihara H, Toda S, Miyabara S, Fujiyama C, Yonemitsu N. Reconstruction of alveolus-like structure from alveolar type II epithelial cells in a three-dimensional collagen gel matrix culture. *Am J Pathol* 1993;**142**:783–92
86. Chakir J, Pagé N, Hamid Q, Laviolette M, Boulet LP, Rouabhia M. Bronchial mucosa produced by tissue engineering: a new tool to study cellular interactions in asthma. *J Allergy Clin Immunol* 2001;**107**:36–40
87. Paquette JS, Moulin V, Tremblay P, Bernier V, Boutet M, Laviolette M, Auger FA, Boulet LP, Goulet F. Tissue-engineered human asthmatic bronchial equivalents. *Eur Cell Mater* 2004;**7**:1–11 (discussion 1–11)
88. Matrosovich MN, Matrosovich TY, Gray T, Roberts NA, Klenk HD. Human and avian influenza viruses target different cell types in cultures of human airway epithelium. *Proc Natl Acad Sci U S A* 2004;**101**:4620–4
89. Birkness KA, Guarner J, Sable SB, Tripp RA, Kellar KL, Bartlett J, Quinn FD. An in vitro model of the luekocyte interactions associated with granuloma formation in Mycobacterium tuberculosis infection. *Immunol Cell Biol* 2007;**85**:160–8
90. Nguyen Hoang AT, Chen P, Juarez J, Sachamitr P, Billing B, Bosnjak L, Dahlén B, Coles M, Svensson M. Dendritic cell functional properties in a three-dimensional tissue model of human lung mucosa. *Am J Physiol Lung Cell Mol Physiol* 2012;**302**:L226–37
91. Booth AJ, Hadley R, Cornett AM, Dreffs AA, Matthes SA, Tsui JL, Weiss K, Horowitz JC, Fiore VF, Barker TH, Moore BB, Martinez FJ, Nicklason LE, White ES. Aceullar normal and fibrotic human lung matrices as a culture system for in vitro investigation. *Am J Respir Crit Care Med* 2012;**186**:866–76
92. Bonvillain RW, Danchuk S, Sullivan DE, Betancourt AM, Semon JA, Eagle ME, Mayeux JP, Gregory AN, Wang G, Townley IK, Borg ZD, Weiss DJ, Bunnell BA. A nonhuman primate model of lung regeneration: detergent-mediated decellularization and initial in vitro recellularization with mesenchymal stem cells. *Tissue Eng Part A* 2012;**18**:2437–52
93. Qasaimeh MA, Ricoult SG, Juncker D. Microfluidic probes for use in life sciences and medicine. *Lab Chip* 2013;**13**:40–50
94. Han C, Pang S, Bower DV, Yiu P, Yang C. Wide field-of-view on-chip Talbot fluorescence microscopy for longitudinal cell culture monitoring from within the incubator. *Anal Chem* 2013;**85**:2356–60
95. Whitesides GM. The origins and the future of microfluidics. *Nature* 2006;**442**:368–73
96. White AK, VanInsberghe M, Petriv OI, Hamidi M, Sikorski D, Marra MA, Piret J, Aparicio S, Hansen CL. High-throughput microfluidic single-cell RT-qPCR. *Proc Natl Acad Sci U S A* 2011;**108**:13999–4004
97. Zhang Z, Nagrath S. Microfluidics and cancer: are we there yet? *Biomed Microdevices* 2013;**15**:595–609
98. Tang T, Badal MY, Ocvirk G, Lee WE, Bader DE, Bekkaoui F, Harrison DJ. Integrated microfluidic electrophoresis system for analysis of genetic materials using signal amplification methods. *Anal Chem* 2002;**74**:725–33
99. Hong JW, Quake SR. Integrated nanoliter systems. *Nat Biotechnol* 2003;**21**:1179–83
100. Winer-Jones JP, Vahidi B, Arquilevich N, Fang C, Ferguson S, Harkins D, Hill C, Klem E, Pagano PC, Peasley C, Romero J, Shartle R, Vasko RC, Strauss WM, Dempsey PW. Circulating tumor cells: clinically relevant molecular access based on a novel CTC flow Cell. *PLoS One* 2014;**9**:e86717
101. Sequist LV, Nagrath S, Toner M, Haber DA, Lynch TJ. The CTC-chip: an exciting new tool to detect circulating tumor cells in lung cancer patients. *J Thorac Oncol* 2009;**4**:281–3
102. Fluidigm Corporation. http://www.mscience.com.au/upload/pages/singlecell/c1_mrna_ brochure-br100-6199-a1.pdf?1391142668
103. Chan MC, Chan RW, Yu WC, Ho CC, Yuen KM, Fong JH, Tang LL, Lai WW, Lo AC, Chui WH, Sihoe AD, Kwong DL, Wong DS, Tsao GS, Poon LL, Guan Y, Nicholls JM, Peiris JS. Tropism and innate host responses of the 2009 pandemic H1N1 influenza virus in ex vivo and in vitro cultures of human conjunctiva and respiratory tract. *Am J Pathol* 2010;**176**:1828–40
104. Zhang L, Bukreyev A, Thompson CI, Watson B, Peeples ME, Collins PL, Pickles RJ. Infection of ciliated cells by human parainfluenza virus type 3 in an in vitro model of human airway epithelium. *J Virol* 2005;**79**:1113–24
105. Chan MC, Chan RW, Yu WC, Ho CC, Chui WH, Lo CK, Yuen KM, Guan YI, Nicholls JM, Peiris JS. Influenza H5N1 virus infection of polarized human alveolar epithelial cells and lung microvascular endothelial cells. *Respir Res* 2009;**10**:102
106. Diebel LN, Liberati DM, Diglio CA, Brown WJ. Immunoglobulin A modulates inflammatory responses in an in vitro model of pneumonia. *J Trauma* 2005;**59**:1099–106
107. Nalayanda DD, Wang Q, Fulton WB, Wang TH, Abdullah F. Engineering an artificial alveolar-capillary membrane: a novel continuously perfused model within microchannels. *J Pediatr Surg* 2010;**45**:45–51
108. Nalayanda DD, Fulton WB, Wang TH, Abdullah F. A multiphase fluidic platform for studying ventilator-induced injury of the pulmonary epithelial barrier. *Integr Biol (Camb)* 2013;**5**:1141–8
109. Zamir M, Moore JE, Fujioka H, Gaver DP. Biofluid mechanics of special organs and the issue of system control. *Ann Biomed Eng* 2010;**38**:1204–15
110. Evangelatov A, Pankov R. The evolution of three-dimensional cell cultures towards unimpeded regenerative medicine. *Regenerative Medicine and Tissue Engineering*. Prof. Jose A Andrades (Ed.) web publication by INTECH OPEN, http://www.intechopen.com/books/regenerative-medicine-and-tissue-engineering/the-evolution-of-three-dimensional-cell-cultures-towards-unimpeded-regenerative-medicine-and-tissue- (2013, accessed on 12 May 2014), ISBN: 978-953-51-1108-5

111. Ingber DE. Tensegrity and mechanotransduction. *J Bodyw Mov Ther* 2008;**12**:198–200
112. Lin YM, Zhang A, Rippon HJ, Bismarck A, Bishop AE. Tissue engineering of lung: the effect of extracellular matrix on the differentiation of embryonic stem cells to pneumocytes. *Tissue Eng Part A* 2010;**16**:1515–26
113. Luque T, Melo E, Garreta E, Cortiella J, Nichols J, Farré R, Navajas D. Local micromechanical properties of decellularized lung scaffolds measured with atomic force microscopy. *Acta Biomater* 2013;**9**:6852–9
114. Shamis Y, Hasson E, Soroker A, Bassat E, Shimoni Y, Ziv T, Sionov RV, Mitrani E. Organ-specific scaffolds for in vitro expansion, differentiation, and organization of primary lung cells. *Tissue Eng Part C Methods* 2011;**17**:861–70
115. Luque T, Melo E, Garreta E, Cortiella J, Nichols J, Farre R, Navajas D. Local micromechanical properties of decellularized lung scaffolds measured with atomic force microscopy. *Acta Biomater* 2013;**9**:6852–9
116. Huh D, Hamilton GA, Ingber DE. From 3D cell culture to organs-on-chips. *Trends Cell Biol* 2011;**21**:745–54
117. Folch A, Toner M. Microengineering of cellular interactions. *Annu Rev Biomed Eng* 2000;**2**:227–56
118. Khademhosseini A, Langer R, Borenstein J, Vacanti JP. Microscale technologies for tissue engineering and biology. *Proc Natl Acad Sci U S A* 2006;**103**:2480–87
119. Liu M, Transwell AK, Post M. Mechanical force-induced signal transduction in lung cells. *Am J Physiol* 1999;**277**:L667–83
120. Schwartz MA. Integrin signaling revisited. *Trends Cell Biol* 2001;**11**:466–70
121. Vogel V, Sheetz MP. Cell fate regulation by coupling mechanical cycles to biochemical signaling pathways. *Curr Opin Cell Biol* 2009;**21**:38–46
122. Lukashev ME, Werb Z. ECM signalling: orchestrating cell behaviour and misbehaviour. *Trends Cell Biol* 1998;**8**:437–41
123. Han B, Lodyga M, Liu M. Ventilator-induced lung injury: role of protein-protein interaction in mechanosensation. *Proc Am Thorac Soc* 2005;**2**:181–7
124. Wang Y, Maciejewski BS, Weissmann G, Silbert O, Han H, Sanchez-Esteban J. DNA microarray reveals novel genes induced by mechanical forces in fetal lung type II epithelial cells. *Pediatr Res* 2006;**60**:118–24
125. Wang Y, Huang Z, Nayak PS, Matthews BD, Warburton D, Shi W, Sanchez-Esteban J. Strain-induced differentiation of fetal type II epithelial cells is mediated via the integrin α6β1-ADAM17/tumor necrosis factor-α-converting enzyme (TACE) signaling pathway. *J Biol Chem* 2013;**288**:25646–57
126. Gossett DR, Tse HTK, Lee SA, Ying Y, Lindgren AG, Yang OO, Rao J, Clark AT, Carlo DD. Hydrodynamic stretching of single cells for large population mechanical phenotyping. *Proc Natl Acad Sci U S A* 2012;**109**:7630–35
127. Polacheck WJ, Li R, Uzel SGM, Kamm RD. Microfluidic platforms for mechanobiology. *Lab Chip* 2013;**13**:2252–67
128. Kim DH, Wong PK, Park J, Levchenko A, Sun Y. Microengineered platforms for cell mechanobiology. *Annu Rev Biomed Eng* 2009;**11**:203–33
129. Goldblum SE, Yoneda K, Cibull M, Pearson T, Hall C, Marshall ME. Human recombinant interleukin-2 provokes acture pulmonary vascular endothelial injury in rabbits. *J Biol Response Mod* 1990;**9**:127–39
130. Matute-Bello G, Frevert CW, Martin TR. Animal models of acute lung injury. *Am J Physiol Lung Cell Mol Physiol* 2008;**295**:L379–99
131. Chen Y, Guo H, Xu D, Xu X, WEang H, Hu X, Lu Z, Kwak D, Xu Y, Gunther R, Huo Y, Weir EK. Left ventricular failure produces profound lung remodeling and pulmonary hypertension in mice: heart failure causes severe lung disease. *Hypertension* 2012;**59**:1170–78
132. Murakami K, Okajima K, Uchiba M, Johno M, Nakagaki T, Okabe H, Takatsuki K. Activated protein C attenuates endotoxin-induced pulmonary vascular injury by inhibiting activated leukocytes in rats. *Blood* 1996;**87**:642–7
133. Berger MM, Rozendal CS, Schieber C, Dehler M, Zugel S, Bardenheuer HJ, Bartsch P, Mairbaurl H. The effect of endothelin-1 on alveolar fluid clearance and pulmonary edema formation in the rat. *Anesth Analg* 2009;**108**:225–31
134. Gross P. Enzymatically produced pulmonary emphysema: a preliminary report. *J Occup Med* 2006;**6**:481
135. Senior RM, Tegner H, Kuhn C, Ohlsson K, Strarcher BC, Pierce JAL. The induction of pulmonary emphysema with human leukocyte elastase. *Am Rev Respir Dis* 1977;**116**:469
136. Atunes MA, Rocco PRM. Elastase-induced pulmonary emphysema: insights from experimental models. *An Acad Bras Cienc* 2011;**83**:1385–95
137. Bánhegyi G, Braun L, Csala M, Puskás F, Mandl J. Ascorbate metabolism and its regulation in animals. *Free Radic Biol Med* 1997;**23**:793–803
138. Huizar I, Malur A, Patel J, McPeek M, Dobbs L, Wingard C, Barna BP, Thomassen MJ. The role of PPARγ in carbon nanotube-elicited granulomatous lung inflammation. *Respir Res* 2013;**14**:7
139. Costa CLB, Spilborghs GMFT, Martins MA, Saldiva PHN, Mauad T. Nitric acid-induced bronchiolitis in rats mimics childhood bronchiolitis obliterans. *Respiration* 2005;**72**:642–9
140. Palmer SM, Flake GP, Kelly FL, Zhang HL, Nugent JL, Kirby PJ, Foley JF, Gwinn WM, Morgan DL. Severe airway epithelial injury, aberrant repair and bronchiolitis obliterans develops after diacetyl instillation in rats. *PloS One* 2011;**6**:e17644
141. Tavana H, Huh D, Grotber JB, Takayama S. Microfluidics, lung surfactant, and respiratory disorders. *Lab Med* 2009;**40**:203–9
142. Barker AF. Bronchiectasis. *N Engl J Med* 2002;**346**:1383–93
143. Reid L. An experimental study of hypersecretion of mucus in the bronchial tree. *Br J Exp Pathol* 1963;**44**:437–45
144. Rogers CS, Stoltz DA, Meyerholz DK, Ostedgaard LS, Rokhlina T, Taft PJ, Rogan MP, Pezzulo AA, Karp PH, Itani OA, Kabel AC, Wohlford-Lenane CL, Davis GJ, Hanfland RA, Smith TL, Samuel M, Wax D, Murphy CN, Rieke A, Whitworth K, Uc A, Starner TD, Brogden KA, Shilyansky J, McCray PB Jr, Zabner J, Prather RS, Welsh MJ. Distruption of the CFTR gene produces a model of cystic fibrosis in newborn pigs. *Science* 2008;**321**:1837–41
145. Stoltz DA, Rokhlina T, Ernst SE, Pezzulo AA, Ostedgaard LS, Karp PH, Samuel MS, Reznikov LR, Rector MV, Gansemer ND, Bouzek DC, Alaiwa MH, Hoegger MJ, Ludwig PS, Taft PJ, Wallen TJ, Wohlford-Lenane C, McMenimen JD, Chen JH, Bogan KL, Adam RJ, Hornick EE, Nelson GA 4th, Hoffman EA, Chang EH, Zabner J, McCray PB Jr, Prather RS, Meyerholz DK, Welsh MJ. Intestinal CFTR expression alleviates meconium ileus in cystic fibrosis pigs. *J Clin Invest* 2013;**123**:2685–93
146. Clarke LL, Grubb BR, Gabriel SE, Smithies O, Koller BH, Boucher RC. Defective epithelial chloride transport in a gene-targeted mouse model of cystic fibrosis. *Science* 1992;**257**:1125–8
147. Snouwaert JN, Brigman KK, Latour Am, Malouf NN, Boucher RC, Smithies O, Koller BH. An animal model for cystic fibrosis made by gene targeting. *Science* 1992;**257**:1083–88
148. Meeks M, Bush A. Primary ciliary dyskinesia (PCD). *Pediatr Pulmonol* 2000;**29**:307–16
149. Craig VJ, Quintero PA, Fyfe SE, Patel AS, Knolle MD, Kobzik L, Owen CA. Profibrotic activities for matrix metalloproteinase-8 during bleomycin-mediated lung injury. *J Immunol* 2013;**190**:4283–96
150. Jiang D, Liang J, Hodge J, Lu B, Zhu Z, Yu S, Fan J, Gao Y, Yin Z, Homer R, Gerard C, Noble PW. Regulation of pulmonary fibrosis by chemokine receptor CXCR3. *J Clin Invest* 2004;**14**:291–9
151. Tager AM, Kradin RL, LaCamera P, Bercury SD, Campanella GS, Leary CP, Polosukhin V, Zhao LH, Sakamoto H, Blackwell TS, Luster AD. Inhibition of pulmonary fibrosis by the chemokine IP-10/CXCL10. *Am J Respir Cell Mol Biol* 2004;**31**:395–404
152. Baron RM, Choi AJS, Owen CA, Choi AM. Genetically manipulated mouse models of lung disease: potential and pitfalls. *AJP-Lung Cell Mol Physiol* 2012;**302**:L485–L97
153. Haston CK, Wan M, Dejournett RE, Zhou X, Ni D, Gu X, King TM, Weil MM, Newman RA, Amos CI, Travis EL. Bleomycin hydrolase and a geneti locus within the MHC affect risk for pulmonary fibrosis in mice. *Hum Mol Genet* 2002;**11**:1855–63
154. Chen Y, Guo H, Xu D, Xu X, Wang H, Hu X, Lu Z, Kwak D, Xu Y, Gunther R, Huo Y, Weir EK. Left ventricular failure produces profound

lung remodeling and pulmonary hypertension in mice: heart failure causes severe lung disease. *Hypertension* 2012;**59**:1170–78
155. Sisson TH, Mendez M, Choi K, Subbotina N, Courey A, Cunningham A, Dave A, Engelhardt JF, Liu X, White ES, Thannickal VJ, Moore BB, Christensen PJ, Simon RH. Targeted injury of type II alveolar epithelial cells induces pulmonary fibrosis. *Am J Respir Crit Care Med* 2010;**181**:254–63
156. Osterholzer JJ, Olsewski MA, Murdock BJ, Chen GH, Erb-Downward JR, Subbotina N, Browning K, Lin Y, Morey RE, Dayrit JK, Horowitz JC, Simon RH, Sisson TH. Implicating exudate macrophages and Ly-Chigh monocytes in CCR2-dependent lung fibrosis following gene-targeted alveolar injury. *Am J Respir Crit Care Med* 2011;**183**:A6148
157. Sayes CM, Reed KL, Warheit DB. Assessing toxicity of fine and nanoparticles: comparing in vitro measurements to in vitro pulmonary toxicity profiles. *Toxicol Sci* 2007;**97**:163–80
158. Zhu Z, Yang G, Wang Y, Yang J, Ai G, Niu P, Tian L. Suppression of thioredoxin system contributes to silica-induced oxidative stress and pulmonary fibrogenesis in rats. *Toxicol Lett* 2013;**222**:289–94
159. Mossman BT, Lippmann M, Hesterberg TW, Kelsey KT, Barchowsky A, Bonner JC. Pulmonary endpoints (lung carcinomas and asbestosis) following inhalation exposure to asbestos. *J Toxicol Environ Health B Crit Rev* 2011;**14**:76–121
160. Liu G, Cheresh P, Kamp DW. Molecular basis of asbestos-induced lung disease. *Ann Rev Pathol Mech Dis* 2013;**8**:161–87
161. Brody AR, Hill LH, Adkins B, O'Connor RW. Chrysotile asbestoas inhalation in rats: deposition pattern and reaction of alveolar epithelium and pulmonary macrophages. *Am Rev Respir Dis* 1981;**123**:670–79
162. Vernath JM, Cutler NS, Kaser EG, Reilly CA, Yost GS. Effects of cell type and culture media on Interleukin-6 secretion in response to environmental particles. *Toxicol In Vitro* 2008;**22**:498–509
163. Yao S, Chen HH, Harte E, Ventura GD, Petibois C. The role of asbestos morphology on their cellular toxicity: an in vitro 3D Raman/Rayleigh imaging study. *Anal Bioanal Chem* 2013;**405**:8701–7
164. Sussman RG, Cohen BS, Lippmann M. Asbestoas fiber deposition in a human tracheobronchial cast I. *Exp Inhal Toxicol* 1992;**3**:145–60
165. Das M, Fessel J, Tang H, West J. A process-based review of mouse models of pulmonary hypertension. *Pulm Circ* 2012;**2**:415–33
166. Gomez-Arroyo JG, Farkas L, Alhussaini AA, Farkas D, Kraskauskas D, Voelkel NF, Bogaard HJ. The monocrotaline model of pulmonary hypertension in perspective. *Am J Physiol Lung Cell Mol Physiol* 2012;**302**:L363–9
167. van Suylen Rj, Smits JF, Daemen MJ. Pulmonary artery remodeling differs in hypoxia- and monocrotaline-induced pulmonary hypertension. *Am J Respir Crit Care Med* 1988;**157**:1423–8
168. Chen Y, Guo H, Xu D, Xu X, Wang H, Hu X, Lu Z, Kwak D, Xu Y, Gunther R, Huo Y, Weir EK. Left ventricular failure produces profound lung remodeling and pulmonary hypertension in mice: heart failure causes severe lung disease. *Hypertension* 2012;**59**:1170–78
169. Ciuclan L, Bonneau O, Hussey M, Duggan N, Holmes AM, Good R, Stringer R, Jones P, Morrell NW, Jarai G, Walker C, Westwick J, Thomas M. A novel murine model of severe pulmonary arterial hypertension. *Am J Respir Crit Care Med* 2011;**184**:1174–82
170. Abe K, Toba M, Alzoubi A, Ito M, Fagan KA, Cool CD, Voelkel NF, McMurtry IF, Oka M. Formation of plexiform lesions in experimental severe pulmonary arterial hypertension. *Circulation* 2010;**121**:2747–54
171. Munster VJ, de Wit E, van den Brand JM, Herfst S, Schrauwen EJA, Bestebroer TM, van de Vijver D, Boucher CA, Koopmans M, Rimmelzwaan GF, Kuiken T, Osterhaus ADME, Fouchier RAM. Pathogenesis and transmission of swine-origin 2009 A(H1N1) influenza virus in ferrets. *Science* 2009;**325**:481–3
172. Kraus TA, Garza L, Horvath CM. Enabled interferon signaling evasion in an immune-competent transgenic mouse model of parainfluenza virus 5 infection. *Virology* 2008;**371**:196–205
173. Jafri HS, Chavez-Bueno S, Mejias A, Gomez AM, Rios AM, Nassi SS, Yusuf M, Kapur P, Hardy RD, Hatfield J, Rogers BB, Krisher K, Ramilo O. Respiratory syncytial virus induces pneumonia, cytokine response, airway obstruction, and chronic inflammatory infiltrates associated with long-term airway hyperresponsiveness in mice. *J Infect Dis* 2004;**189**:1856–65
174. Rimmelzwaan GF, Kuiken T, van Amerongen G, Bestebroer TM, Fouchier RA, Osterhaus AD. Pathogenesis of influenza A (H5N1) virus infection in a primate model. *J Virol* 2001;**75**:6687
175. Calderon VE, Valbuena G, Goez Y, Judy BM, Huante MB, Sutjita P, Johnston RK, Estes DM, Hunter RL, Actor JK, Cirillo JD, Endsley JJ. A humanized mouse model of tuberculosis. *PLoS One* 2013;**8**:e63331
176. Villenave R, Thavagnanam S, Sarlang S, Parker J, Douglas I, Skibinski G, Heaney LG, McKaigue JP, Coyle PV, Shields MD, Power UF. In vitro modeling of respiratory syncytial virus infection of pediatric bronchial epithelium, the primary target of infection in vivo. *Proc Natl Acad Sci U S A* 2012;**109**:5040–5
177. van den Brand JM, Stittelaar KJ, Leijten LM, van Amerongen G, Simon JH, Osterhaus AD, Kuiken T. Modification of the ferret model for pneumonia from seasonal human influenza A virus infection. *Vet Pathol* 2012;**49**:562
178. Tateda K, Takashima K, Miyazaki H, Matsumoto T, Hatori T, Yamaguchi K. Noncompromised penicillin-resistant pneumococcal pneumonia CBA/J mouse model and comparative efficiencies of antibiotics in this model. *Antimicrob Agents Chemother* 1996;**40**:1520–5
179. Xu L, Bao L, Dend W, Zhu H, Chen T, Lv Q, Li F, Yuan J, Xiang Z, Gao K, Xu Y, Huang L, Li Y, Liu J, Yao Y, Yu P, Yong W, Wei Q, Zhang L, Qin C. The mouse and ferret models for studying the novel avian-origin human influenza A (H7N9) virus. *Virol J* 2013;**10**:253
180. Saladino RA, Stack AM, Fleisher GR, Thompson CM, Briles DE, Kobzik L, Siber GR. Development of a model of low-inoculum streptococcus pneumonia intrapulmonary infection in infant rats. *Infect Immun* 1997;**65**:4701–4
181. Reed DS, Smith L, Dunsmore T, Trichel A, Ortiz LA, Cole KS, Barry E. Pneumonic tularemia in rabbits resembles the human disease as illustrated by radiographic and hematological changes after infection. *PLoS One* 2001;**6**:e24654
182. Hooper JW, Larsen T, Custer DM, Schmaljohn CS. A lethal disease model for hantavirus pulmonary syndrome. *Virology* 2001;**289**:6–14
183. Roberts A, Paddock C, Vogel L, Butler E, Zaki S, Subbarao K. Aged BALB/c mice as a model for increased severity of severe acute respiratory syndrome in elderly humans. *J Virol* 2005;**79**:5833–8
184. de Wit E, Rasmussen AL, Falzarano D, Bushmaker T, Feldmann F, Brining DL, Fischer ER, Martellaro C, Okumura A, Chang J, Scott D, Benecke AG, Katze MG, Feldmann H, Munster VJ. Middle east respiratory syndrome coronavirus (MERS-CoV) causes transient lower respiratory tract infection in rhesus macaques. *PNAS* 2013;doi:10.1073/pnas.1310744110
185. Yen YT, Liao F, Hsiao CH, Kao CL, Chen YC, Wu-Hsieh BA. Modeling the early events of severe acute respiratory syndrome coronavirus infection in vitro. *J Virol* 2006;**80**:2684–93
186. Zhou J, Chu H, Li C, Wong BH, Cheng ZS, Poon VK, Sun T, Lau CC, Wong KK, Chan JY, Chan JF, To KK, Chan KH, Zheng BJ, Yuen KY. Active MERS-CoV replication and aberrant induction of inflammatory cytokines and chemokines in human macrophages: implications for pathogenesis. *J Infect Dis* 2013;doi: 10.1093/infdis/jit504
187. Jungraithmayr W, Draenert A, Marquardt K, Weder W. Ultrastructural Changes in acute lung allograft rejection: novel insights from an animal study. *J Heart Lung Transplant* 2012;**31**:94–100
188. Cotran RS. American Association of Pathologists president's address. New roles for the endothelium in inflammation and immunity. *Am J Pathol* 1987;**129**:407–13
189. Baluna R, Vitetta ES. Vascular leak syndrome: a side effect of immunotherapy. *Immunopharmacology* 1997;**37**:117–32
190. Rosenstein M, Ettinghausen SE, Rosenberg SA. Extravasation of intravascular fluid mediated by the systemic administration of recombinant interleukin 2. *J Immunol* 1986;**137**:1735–42
191. Conant EF, Fox KR, Miller WT. Pulmonary edema as a complication of interleukin-2 therapy. *AJR Am J Roentgenol* 1989;**152**:749–52
192. Mossman BT, Lippmann M, Hesterberg TW, Kelsey KT, Barchowsky A, Bonner JC. Pulmonary endpoints (Lung carcinomas and asbestosis) following inhalation exposure to asbestos. *J Toxicol Environ Health Part B* 2011;**14**:76–121
193. Ervin MH. A simple low-vacuum environmental cell. *Microsc Microanal* 2003;**9**:18–28

194. Valberg PA, Bruch J, McCunney RJ. Are rat results from Intratracheal instillation of 19 granular dusts a reliable basis for predicting cancer risk? *Regul Toxicol Pharmacol* 2009;**54**:72–83
195. Veranth JM, Cutler NS, Kaser EG, Reilly CA, Yost GS. Effects of cell type and culture media on Interleukin-6 secretion in response to environmental particles. *Toxicol In Vitro* 2008;**22**:498–509
196. Sussman RG, Cohen BS, Lippmann M. Asbestos fiber deposition in a human tracheobronchial cast. *I Exp Inhal Toxicol* 1991;**3**:145–60
197. Seydou Y, Chen HH, Harte E, Ventura GD, Petibois C. The role of asbestos morphology on their cellular toxicity: an in vitro 3D Raman/Rayleigh imaging study. *Anal Bioanal Chem* 2013;**405**:8701–7
198. Tsuda A, Stringer BK, Mijailovich SM, Rogers RA, Hamada K, Gray ML. Alveolar cell stretching in the presence of fibrous particles indues interleukin-8 responses. *Am J Respir Cell Mol Biol* 1999;**21**:455–62
199. van der Worp HB, Howells DW, Sena ES, Porritt MJ, Rewell S, O'Collins V, Macleod MR. Can animal models of disease reliably inform human studies? *PLoS Med* 2010;**7**:e1000245
200. Yen YT, Liao F, Hsiao CH, Kao CL, Chen YC, Wu-Hsieh BA. Modeling the early events of severe acute respiratory syndrome coronavirus infection in vitro. *J Virol* 2006;**80**:2684–93
201. Cordes N, Blaese MA, Plasswilm L, Rodemann, Van Beuningen D. Fibronectin and laminin increase resistance to ionizing radiation and the cyotoxic drug Ukrain in human tumour and normal cells in vitro. *Int J Radiat Biol* 2003;**79**:709–20
202. Al-Batran SE, Astner ST, Supthut M, Gamarra F, Brueckner K, Welsch U, Knuechel R, Huber RM. Three-dimensional in vitro cocultivation of lung carcinoma cells with human bronchial organ culture as a model for bronchial carcinoma. *Am J Respir Cel Mol Biol* 1999;**21**:200–8
203. Hanahan D, Weinberg RA. The hallmarks of cancer. *Cell* 2000;**100**:57–70
204. Kwon M, Berns A. Mouse models for lung cancer. *Mol Oncol* 2013;**7**:165–77
205. Zheng MF, Shen SY, Huang WD. DCA increases the antitumor effects of capecitabine in a mouse B16 melanoma allograft and a human non-small cell lung cancer A549 xenograft. *Cancer Chemother Pharmacol* 2013;**72**:1031–41
206. Pilewski JM, Bumbalo TS, Davis AG, Siegfried JM. Hepatocyte growth factor promotes tumor growth in a novel in vivo model of human lung Cancer. *Am J Respir Cell Mol Biol* 2001;**24**:556–62
207. Moro M, Bertolini G, Tortoreto, Pastorino U, Sozzi G, Roz L. Patient-derived xenografts of non small cell lung cancer: resurgence of an old model for investigation of modern concepts of tailored therapy and cancer stem cells. *J Biomed Biotechnol* 2012; Article ID 568567 doi:10.1155/2012/568567
208. Cordes N, Blaese MA, Plasswilm L, Rodemann, Van Beuningen D. Fibronectin and laminin increase resistance to ionizing radiation and the cyotoxic drug Ukrain in human tumour and normal cells in vitro. *Int J Radiat Biol* 2003;**79**:709–20